ASSESSMENT OF THE EXISTING MODELS TO EVALUATE THE SHEAR STRENGTH CONTRIBUTION OF EXTERNALLY BONDED FRP SHEAR REINFORCEMENTS

Eva Oller*, Renata Kotynia**, Antonio Marí*

*Universitat Politècnica de Catalunya, Barcelona, Spain

**Lodz University of Technology, Lodz, Poland

Corresponding author:

Eva Oller, e-mail: eva.oller@upc.edu, Phone (+34) 93 401 65 12

ABSTRACT

This paper presents an analysis of the performance of different existing formulations to quantify the FRP contribution to the shear strength of RC elements strengthened in shear by externally bonded FRP sheets. A large database of 555 tests has been assembled distinguishing between the shape of the section, the existence of internal transverse reinforcement and the FRP configurations. In general, predictions are more conservative for beams without transverse reinforcement. In addition, in some cases predictions are unsafe for beams with transverse reinforcement, showing a possible interaction with the internal transverse reinforcement which is not considered in the experimental FRP contribution to the shear strength. For wrapped FRP configurations, models generally assumed failure at the bottom corner of the section and results are very conservative in some cases where failure was experimentally observed along the web. For U-shaped and side-bonded configuration, results depend mainly on the assumed bond model and are more accurate than in the previous case, showing for some models unsafe predictions for the continuous FRP system applied in beams with transverse reinforcement.

Keywords: shear strength, stress transfer, analytical modelling, EB FRP reinforcement.

1. INTRODUCTION

Nowadays, there is still a lack of worldwide consensus on the evaluation of the shear strength contribution of the externally bonded (EB) fibre reinforced polymer (FRP) reinforcement, in elements strengthened in shear through this technique. This is due to the confluence of many different reasons: a) the complexity of the shear phenomenon; b) the debonding of the external reinforcement for some configurations and its prediction, c) the linear elastic behaviour of the FRP material (the EB FRP stirrups do not yield); and d) the interaction between concrete, internal steel transverse reinforcement if it exists, the longitudinal reinforcement, and the EB FRP reinforcement.

The EB FRP shear strengthening can be performed in different configurations: a) sheets fully wrapping the section (wrapped); b) sheets or L-shaped laminates bonded on the lateral sides and the bottom surface of the beam (U-shaped); and c) sheets or laminates bonded in the lateral sides of the section (side-bonded). The sheets and laminates can be bonded in a continuous or discontinuous configuration. Both U-shaped and side-bonded configurations are susceptible of debonding once a critical shear crack opens and widens. Then, if the bonded length of each strip at the upper side of the crack (for the U-shaped) or at both sides of the crack (for the side-bonded case) is not long enough to anchor the tensile force of the FRP, the laminate debonds suddenly before reaching its ultimate capacity. This debonding failure mode can be delayed or can be avoided by using appropriate anchorage devices.

The ultimate shear strength of beams externally strengthened in shear by FRP laminates can be calculated as the sum of the contribution of the different components: concrete, transverse steel and FRP external reinforcement.

Some of the existing guidelines (fib Bulletin 90 [1], ACI440.2R-17 [2], CNR-DT-200/2013-R1 [3], Concrete Society TR-55 [4], DAfStb Heft 595 [5], fib Bulletin 14 [6]) add the contribution of the externally bonded (EB) FRP reinforcement to the shear strength of the unstrengthened element. This approach has been previously discussed by [7,8], [9] and [10,11] observing that the presence of the FRP could influence the effective stress in the internal steel, sometimes leading to non-conservative results. This might be due to possible changes in the strut orientation or additional cracking that may change the contribution of the concrete or existing transverse reinforcement to the shear strength. The interaction of the FRP shear reinforcement with the transversal steel or the concrete is only considered in a few number of the existing formulations (Modifi and Chaallal [12], Monti and Liotta [13], Kotynia [14]; Colotti [15]; Ali et al. [16]; Petrone and Monti [17]). Bousselham and Chaallal in [8] concluded that the contribution of concrete remains more or less unchanged after the formation of diagonal cracking for small and medium size beams. In addition, according to Bousselham and Chaallal [8], the FRP has a significant influence on the behaviour of the transverse steel. In the case of beams with transverse stirrups, the transverse steel contribution is higher than that of FRP, due to better bonding at the stirrup-concrete interface. According to Pellegrino and Modena [18], Deniaud and Cheng [19], Monti and Liotta [13], and Ali et al. [16], the interaction between transverse steel and FRP is important since there is not always full interaction between the shear capacity of the steel stirrups and the FRP, that is, the system is not ductile enough to allow that the maximum contribution of each material occurs at the same instant. Ali et al. [16] developed a partial-interaction mathematical model which was not considered in the following study due to its complexity to be applied in a large database. Mofidi and Chaallal [20] performed a study of the major factors affecting the shear contribution of the FRP, concluding that even though none of the existing guidelines explicitly consider the transverse internal steel contribution when calculating the FRP shear strength, it has a significant influence. In addition, Mofidi and Chaallal in [21] concluded that a lower contribution of existing steel stirrups (due to non-yielding) instead of the full contribution considered in the existing recommendations depends on the stirrup spacing. For this reason, some of the existing recommendations are very strict in detailing to take this fact into account. Colotti et al. [22] developed a closed-form analytical solution for quantifying the contribution of steel stirrups and FRP strips by integrating the stress distributions along the beam height as the critical crack widens. This formulation provides a peak value of the combined contribution of both materials steel and FRP. The FRP contribution follows the same treatment to that used by Chen and Teng [23] but with another bond strength model.

The existing guidelines provide formulations to evaluate the shear strength contribution of the FRP laminates (V_f) which are similar to the contribution of the internal transverse steel reinforcement to the shear strength (Eq. (1)), since most of them are based on the truss analogy.

$$V_f = \frac{A_f}{s_f} \cdot z_f \cdot f_{fd} \cdot \left(\cot\theta + \cot\alpha \right) \cdot \sin\alpha \tag{1}$$

where A_f/s_f is the area per unit length of FRP reinforcement, z_f is the inner lever arm of the FRP reinforcement, f_{fd} is the FRP design tensile strength when failure occurs, θ is the angle between the concrete compression strut and the longitudinal axis of the member, α is the angle between principal fibre orientation of the FRP and the longitudinal axis of the member.

The definition of the stress level at the FRP and the θ angle are the main difference between the existing formulations and guidelines. The effective stress or strain of the FRP is substantially lower than the FRP ultimate strength or strain, this is due to the variable tensile stress developed along the crack profile (Monti and Liotta [13]). Some of the formulations adopt 45º for the θ angle [2,6], or alternatively a variable angle approach [3,5] as that of Eurocode 2 [24].

The main difference with the transverse internal steel formulations is that the FRP reinforcement does not yield at failure. The different existing models define the stresses at the EB reinforcement depending on its configuration, taking into account debonding for the U-shaped and side-bonded configurations and assuming failure in the laminate in the rounded corner of the sections for the wrapped configuration. In other words, they consider different scenarios related to failure. To consider debonding, the anchorage of the FRP laminate in relation to the critical shear crack should be defined. Therefore, some formulations consider a mean value for the bonded length that crosses the critical shear crack. For the wrapped configuration, to consider failure at the rounded corner, most of the formulations are semiempirical and come from an adjustment of a formula obtained from confinement tests performed in columns strengthened with FRP sheets.

Sas et al. [25], Pellegrino and Vasic [11], Rousakis et al. [26] and D'Antino and Triantafillou [27] performed an assessment of the existing formulations to evaluate the FRP shear strength contribution. Sas et al. [25] compared the performance of the formulations of Chaallal [28], Triantafillou [29] and Triantafillou and Antanopoulos [30], Khalifa et al. [31] and Khalifa and Nanni [32], Chen and Teng [33] [23] [34], Deniaud and Cheng [35,36], Adhikary et al. [37], Ye et al. [38], Cao et al. [39], Zhang and Hsu [40], Carolin [41], Carolin and Täljsten [42], and Monti and Liotta [13]. They concluded that the different predictive performance of the models can partially be explained by the fact that some of them were calibrated from a reduced amount of experimental results. According to Sas et al. [25], the shear models for FRP strengthening in the present form do not predict the shear failure very well, and the T-sections were treated as a special case of a rectangular beam. Pellegrino and Vasic [11] analysed the overall shear strength of FRP strenghenend elements, by applying different fomulations to evaluate the FRP shear strength (fib Bulletin 14 [6], CNR-DT-200/2004 [43], ACI440.2R-08 [44], Chen and Teng [23] [34], Carolin and Täljsten [42], Pellegrino and Modena [18], Bukhari et al. [45] and Mofidi and Chaallal [12]) combined with the estimation of the concrete, steel and compressive strength of concrete according to basic model codes for unstrengthened RC structures (Eurocode 2 [24], ACI 318 [46] and Model Code 2010 [47]). In their study, Pellegrino and Vasic [11] focused special attention to the θ angle, which has a significant influence on the prediction of the results. In general, according to Pellegrino and Vasic [11] the CNR-DT-200/2004 [43] and Pellegrino and Modena [18] gave good results in terms of mean value (MV) and coefficient of variation (COV) of the ratio between the experimental and theoretical ultimate shear force. When combining the model of Pellegrino and Modena [18] with the

Eurocode 2 [24], the best predictions were obtained for a variable crack shear angle. Rousakis et al. [26] also performed an assessment and improvement of existing recommendations for shear design of RC beams strengthened with composite materials. In [26], a straightforward comparison of the total shear strength not only the FRP contribution is analysed, observing that the trend line of predictions without safety factors is conservative for most of the existing guidelines. Finally, D’Antino and Triantafillou in [27] performed an assessment of five design guidelines (EN 1998-3 [48], ACI 440.2R-08 [44], DafStb [5], TR-55 [4], CNR-DT/200-R1. 2013[49]) and a new proposed model. They concluded that all models tend to underestimate the FRP shear strength for the completely wrapped configuration. However, models were more accurate for the U-shaped configuration. Their proposal is an extension of the German guideline [5] and gave conservative results (MV=1.77 COV=2.21 for U-shaped and MV=3.51 and COV=4.32 for wrapped).

In this paper, a comparative analysis of the existing formulations to evaluate the FRP contribution (given in Appendix 1) is performed and presented through the use of a wide database of experimental tests distinguishing those cases with and without internal steel transverse reinforcement and the different FRP strengthening configurations.

2. EXPERIMENTAL DATABASE

2.1. Description of the database

A database of 555 RC beams FRP-strengthened, tested and failing in shear has been assembled as seen in Appendix 2 (355 with rectangular section and 200 with T-section). The database gathers the results of more than 80 experimental programs. This database includes tests of other existing available databases such as Dabasum (University of Minho) and the database published in [10, 21, 22, 25]. Despite some of the data belong to existing databases, all data included in this database have previously been checked against the original source.

Beams with the shear span to effective depth ratio (*a/d*) lower than 2.5 (99 beams) were not included in the analysis of the database performed in the following sections to avoid the arch effect. Selected beams with *a/d* higher than 2.5 were well-documented, and had a rectangular (276) or a T (180) cross-section, were externally strengthened in a wrapped (71 R+68 T), U-shaped (114 R+98 T) or side bonded (91 R+14 T) configuration with FRP wet lay-up or pultruded laminates in a continuous or discontinuous manner, and were with or without internal transverse steel reinforcement.

Table 1 summarizes the number of tests included in each subgroup and the main characteristics in distinguishing between the rectangular and the T-sections for those tests with $a/d \geq 2.5$. T-sections with a side-bonded configuration were not considered for the statistical analysis since only few specimens were strengthened by this technique.

Table 1. Number of tests with $a/d \geq 2.5$ included in each of the groups considered in the comparative analysis.

Geometrical parameters obtained from tests and reported in the original papers have been considered for calculating the predictions of each model. Mean values of the material properties have been considered. Partial safety factors have not been included in the calculations of the predictions. Those beams with a U-shaped configuration but with external anchorage devices to avoid laminate debonding were considered as fully wrapped. In [50], the authors have analysed the observed experimental results and the influence of some parameters on the shear performance such as the strengthening configuration, the shear span-to-depth ratio (a/d), the existing steel transverse reinforcement ratio (ρ_{sw}), the concrete strength (f_{ck}), the size effect (d), and the longitudinal reinforcement ratio (ρ_{sL}). Appendix 2 compiles the main data of all analysed tests.

3. EXISTING MODELS TO EVALUATE THE FRP CONTRIBUTION TO THE SHEAR STRENGTH OF EB FRP SHEAR STRENGTHENED BEAMS

The models considered in the comparative analysis of the following section are those included in the existing guidelines (JSCE [51], fib Bulletin 14 [6], CIDAR (2006) [52], TR-55 [4], CNR-DT 200.R1 2013 [49], Dafstb [5], ACI 440.2R-17 [2], fib Bulletin 90 [1]) and also some other approaches such as Rousakis et al. [26], Kotynia [14], Mofidi and Chaallal [20], Pellegrino and Modena [10,18,53], Monti and Liotta [13], Carolin and Täljsten [42] and Chen and Teng [23,34]. In relation to the existing guidelines, the formulation of the Fib Bulletin 14 [6] is based on Triantafillou and Antonopoulos [30], the ACI 440.2R-17 [2] model is based on a research study by Khalifa et al. [31], and the CIDAR (2006) [52] on Chen and Teng [34]. The Italian provisions of the CNR-DT 200/2004 [43], have been updated in the CNR-DT 200 R1.2013 and are based on Monti et al. [54]. Therefore, to avoid similar results these original formulations were not considered in this study except if some significant changes are observed between the original formulation and the guideline. Appendix 1 summarizes the formulation of each model.

The model of Kotynia [14] was slightly improved in this study in relation to the model described in Appendix 1. For instance, the bond model of Bilotta et al. [55] was adopted for the U-shaped and side-bonded cases and the *k* coefficient of the wrapped configurations was modified as follows: k=0.45 for discontinuous configurations and k=0.30 for continuous configurations.

In addition, Table 2 summarizes some of the particularities of each model: the inclusion or not of different FRP strengthening configurations, the adopted value of the theta angle, and the codes for evaluating the concrete and transverse steel capacity.

Table 2. Particularities of the models considered in the comparative analysis.

4. ASSESSMENT OF THE EXISTING FORMULATIONS TO EVALUATE THE FRP CONTRIBUTION TO THE SHEAR STRENGTH OF EB FRP SHEAR STRENGTHENED BEAMS

The reliability of the existing formulations to evaluate the shear strength contribution of the EB FRP of a shear-strengthened RC beam is evaluated in this section through the comparison of the experimental ($V_{f,exp}$) and theoretical ($V_{f,th}$) EB FRP shear contribution at failure. The experimental value of the FRP contribution, $V_{f,exp}$, is calculated as the difference between the ultimate shear force of the strengthened beam and the ultimate shear force of the unstrengthened control beam. Therefore, in this case, it is assumed that there is not an interaction between the shear strength mechanisms due to the presence of the internal steel transverse reinforcement.

Tables 3 to 7 summarize the statistical results in terms of mean value (MV) and coefficient of variation (COV) for the ratio $V_{f,exp}/V_{f,th}$ in RC beams with a rectangular or T-section in a wrapped, U-shaped and side-bonded configuration, with and without internal transverse steel reinforcement, distinguishing in between continuous and discontinuous strengthening systems.

If the mean value of the experimental-to-theoretical ratio, $V_{f,exp}/V_{f,th}$ is higher than 1.0, the theoretical model is conservative and underestimates the resisting capacity of the strengthened section. The mean value is used as a measure of the conservative bias of the procedure. The coefficient of variation, which is the ratio between the standard deviation and the mean value, is a relative measure of accuracy and sample variability. The more homogeneous the sample, the smaller the coefficient of variation. The best model should have the mean ratio close to 1.0 and a low coefficient of variation.

The number of tests analysed for each formulation is not always the same since some of them were not developed for certain cases (i.e. DAfStb [5] does not consider side bonded or inclined strips).

It is assumed a strut inclination angle θ of 45° for all the formulations, when this angle is not defined by the model. A detailed study of this parameter is performed in section 5.

4.1 Wrapped FRP configuration

As observed in Table 3, for the rectangular RC beams without transverse reinforcement and strengthened in a wrapped configuration, all the formulations for V_f show a significant dispersion with coefficients of variation between 30% and 60%, and the existing guidelines show conservative mean values higher than 2.0 in most cases. This fact might be due to the definition of the tensile strength of the FRP that has an upper limit due to the possible failure at the round corner. This limit is the ultimate tensile strength of the FRP multiplied by a factor, which in most cases is very conservative. For instance, according to the DAfStb [5], for round corners of 20 mm (slightly lower than the concrete cover) the factor that multiplies the FRP tensile strength is k_R, which in this case is 0.28, affected by another factor related to long term loading (0.75), that gives 20.83% of the ultimate strength of the laminate. Alternatively, some other guidelines or formulations [4,44] limit the strain of the FRP to 0.004. According to ACI440.2R-17 [2], the strain should also be lower than 0.75 times the ultimate strain of the FRP. The experimental results showed that in 19 out of 29 tests w/o internal transverse steel failure did not initiate at the bottom corner of the section, in 4 out of 29 tests failure was observed at the bottom corner, and in the remaining tests, the failure location was not clearly described.

Despite TR-55 [4] provisions are only valid if the strain in the FRP is greater than the transverse steel reinforcement yielding, there were also applied in this particular case without transverse reinforcement.

For the cases without internal transverse reinforcement, the performance of all models is similar for both continuous and discontinuous configurations. In general, all models are more conservative for the discontinuous cases. The fib Bulletin 14 [6] shows the best statistical performance with a MV of 1.03 and a COV of 37% for the discontinuous configuration and a MV of 1.09 and a COV if 27% for the continuous configuration. Since the fib Bulletin does not consider the GFRP wrapped cases (9 tests instead of 12 tests analysed), the JSCE (2000) and Kotynia (2011) [14] show also a good performance in terms of MV and COV for the 12 tests analysed.

Table 3 also shows the statistical results for the rectangular wrapped RC beams with transverse reinforcement. As generally observed, for the discontinuous configuration, the mean value of the ratio $V_{f,exp}/V_{f,th}$ is less conservative than in the previous case and it is close to 1.0 for some of the models. The coefficient of variation ranges between 20 and 50%. In this case, the fib Bulletin 14 [6] and the modified model of Kotynia [14] show the best performance in terms of MV and COV. For the continuous configuration, the models are in general less conservative with higher coefficients of variation ranging between 30 and 70%. As observed, the fib Bulletin 14 [6] and the modified model of Kotynia [14] show an unsafe mean value (0.72 and 0.80 respectively), in the last case with the lowest coefficient of variation (31%). Then, the DAfStb [5] (MV=1.13, COV=39%) and the CNR-DT/200R1-2013 [3] (MV=1.03, COV=43%) show the best performance for continuous systems in beams with transverse reinforcement.

In relation to the experimental results, for the specimens with rectangular section without transverse reinforcement, the percentage of the experimental FRP shear strength in relation to the total experimental ultimate strength ranges between 20 and 68% with a mean value of 45% and a COV of 27%. For the specimens with transverse reinforcement, the percentage of the FRP contribution ranges between 16 and 58% with a mean value of 38% and a COV of 30%. Therefore, the FRP contribution is higher in the beams without transverse reinforcement.

Table 3. Statistical results of the experimental to theoretical V_f for rectangular RC beams in a wrapped configuration w/o and w/ transverse reinforcement ($a/d \geq 2.5$).

Table 4 shows the statistical results for the cases with T-sections. As observed, the scatter is larger than in the case of rectangular sections, especially for beams with transverse reinforcement. For beams without transverse reinforcement and in a continuous configuration, all models except Fib Bulletin 90 [1], Rousakis et al. [26] and Carolin and Täljsten [42] show an unsafe MV lower than 1.0. The COV ranges between 55-75% which is very high for the number of tests analysed (10). These 10 tests analysed were strengthened in a U-shaped configuration with anchorages in the bottom of the flanges. Failure in these cases was due to anchor pull out attributed to the propagation of diagonal shear cracks to the intersection of the web and flange. Therefore, it might not be appropriate to apply the formulation for wrapped cases to this particular situation where failure is not starting at the bottom corner of the section. The same explanation can be extended to all cases with transverse reinforcement and continuous FRP.

In relation to the experimental results, for the T-sections, without transverse reinforcement, the percentage of FRP contribution ranges between 12 and 59% with a mean value of 37% and a COV of 39%, and with transverse reinforcement it ranges between 4 and 54% with a mean value of 27% and a COV of 43%. In this last case, 4 out of 50 tests show an FRP contribution to the total shear strength lower than 10%. As observed, the variability of the FRP contribution is larger for the T-sections than for the rectangular sections, especially when there is internal transverse reinforcement.

In relation to TR-55 [4], results in Table 3 and 4 do not consider the previously mentioned condition of having an FRP strain higher than the transverse steel yielding strain. When considering this situation, for the cases with transverse reinforcement the results are quite similar for both rectangular and T-sections. A MV=2.53 and a COV=42% is obtained for the 25 rectangular beams with discontinuous FRP and a MV=2.84 and a COV=49% for the 23 T-sections with discontinuous FRP and yielded stirrups. Results do not vary for the continuous configuration, since the internal steel is always yielded at failure.

Table 4. Statistical results of the experimental to theoretical of V_f for RC beam with a T-section in a wrapped configuration w/o and w/ transverse reinforcement ($a/d \geq 2.5$).

4.2 U-shaped FRP configuration

For the U-shaped and side-bonded configurations, the difference between the existing models arise on the definition of debonding. Most of them define a bonded length in relation to the critical shear crack and the FRP strength relies on the debonding initiation point. One of the most exact procedure seems to be that of Kotynia [14], since it calculates the FRP contribution to the shear strength as the sum of the maximum shear stress transferred by all the strips that cross the critical shear crack assuming different positions of the strips in relation to the crack. However, this procedure is not simple for hand calculations. A simpler procedure is defined in some of the remaining guidelines or models, where instead of calculating the contribution of each FRP strip, a mean bonded strength is considered, which also seems reasonable for daily engineering practice.

For the cases without transverse reinforcement (see Table 5) regardless the FRP configuration, fib Bulletin 14 [6] shows the best performance performance in terms of MV and COV, followed by Chen and Teng [34], Kotynia [14] and the DAfStb [5] models. For continuous FRP reinforcement, the TR-55

[4] gives also good results (MV=1.07, COV=36%) in addition to the fib Bulletin 90 [1] (MV = 1.12, COV=35%). The remaining formulations to evaluate the FRP shear strength contribution give in general more conservative mean values. Despite the JSCE [51] shows a good performance for the wrapped cases, it gives a MV significantly lower than 1.0 for the U-shaped configuration. Mofidi and Chaallal [20] shows a good performance for the continuous case (MV=1.19, COV=28%), but a slightly unsafe mean value (0.82) for the discontinuous system.

For the tests with transverse reinforcement (see Table 5), the dispersion is much higher than for tests without transverse reinforcement when evaluating V_f, following the same trend as for the wrapped configuration. All models behave in a similar manner as observed in Table 5 except for the fib Bulletin 90 [1], fib Bulletin 14 [6] and the JSCE [51], all of them with unsafe MV (0.85, 0.68, and 0.38 respectively for discontinuous configurations; and 0.53, 0.51, and 0.19 respectively for continuous configurations). In general, the COV oscillates between 50 and 95% and between 43 and 61% for the discontinuous and continuous cases, respectively. The higher dispersion might be explained by the possible interaction of the FRP shear reinforcement with the shear strength component of the existing transverse reinforcement. The application of an FRP implies an increase of the transverse reinforcement that may modify the inclination of the struts and also the contribution of the internal steel reinforcement to the total shear strength, which is not considered in the calculation of $V_{f,exp}$.

As observed in Table 5, for the cases with transverse reinforcement, Mofidi and Chaallal [20] shows the best performance for both discontinuous (MV=1.17 COV=51%) and continuous EB FRP (MV=1.02 COV=43%), followed by Chen and Teng [34] (MV=0.96, COV=54%). It should also be mentioned that for the continuous cases, most of the formulations give unsafe mean values, ranging between 0.50-0.80. In this particular case, Kotynia [14] shows also one of the best results (MV=0.99, COV=50%).

In relation to the experimental results for rectangular sections and the U-shaped configuration without transverse reinforcement, the percentage of the contribution of the experimental FRP shear strength in relation to the experimental ultimate strength ranges between 26 and 63% with a mean value of 47% and a COV of 21%. For the specimens with transverse reinforcement, the percentage of the FRP contribution ranges between 2 and 46% with a mean value of 24% and a COV of 49%. From these percentages, it can be concluded that the FRP contribution is much lower when having internal transverse reinforcement. In addition, the variability of the EB FRP is also related to a higher scatter on the comparison of the experimental to theoretical prediction.

Table 5. Statistical results of the experimental to theoretical V_f for rectangular RC beams in a U-shaped configuration w/o and w/ transverse reinforcement ($a/d \geq 2.5$).

Table 6 shows the statistical results for T-sections in a U-shaped configuration. In general, the trend of the different formulations is quite similar to the rectangular sections for both cases with and without transverse reinforcement. In general, all sets (with or without transverse reinforcement, discontinuous or continuous configuration) show a large scatter. For the specimens without transverse reinforcement and with a continuous configuration, the scatter of fib Bulletin 90 [1], TR-55 [4], Rousakis et al. [26], Cheng and Teng [34], is mainly due to some experimental programs where the stresses in the FRP are very low due to its total strength which ranges from 170 to 200 MPa. When these cases are not considered, the MV and COV decreases to MV=0.72 and COV 38% for fib Bulletin 90 [1], MV=0.72 and COV=44% for TR-55 [4], MV=1.65 and COV=49% for Rousakis et al. [26], MV=0.82 and COV=48% for Chen ad Teng [34].

For the T-sections, without transverse reinforcement, the percentage of FRP contribution ranges between 10 and 61% with a mean value of 36% and a COV of 34%, and with transverse reinforcement it ranges between 1 and 48 % with a mean value of 18% and a COV of 83%. In this last case, 35 out of 63 tests show an FRP contribution to the total shear strength lower than 10%.

When considering the condition of calculating the TR-55 provisions only for those cases where debonding or failure occurs after transverse steel yielding, for the 34 rectangular specimens with discontinuous FRP strips accomplishing the condition the MV is 1.14 with a COV of 68%, and for the 31 tests with a continuous configurations, the MV is 0.51 and the COV, 48%. For the discontinuous configuration of T-sections, 29 tests accomplished the yielding condition, with a MV of 1.23 and a COV of 16%, and for the continuous configuration the 12 tests accomplishing the condition, the MV was 1.16 and the COV was 65%. Therefore, the statistical performance improves considerably.

Table 6. Statistical results of the experimental to theoretical of V_f for RC beam with a T-section in a U-shaped configuration w/o and w/ transverse reinforcement ($a/d \geq 2.5$).

4.3 Side-bonded FRP configuration

The analysis for the side-bonded configuration in rectangular beams with and without transverse reinforcement is presented in Table 7. When evaluating V_f and for beams without transverse reinforcement, Chen and Teng [34] shows the best performance for the discontinuous configuration (MV=1.01, COV=46%). However, for the continuous configuration, Kotynia [14] (MV=0.99, COV=56%) and Carolin and Täljsten [42] (MV=1.07, COV= 57%) behave better than Chen and Teng (2003) [34] (MV=1.47, COV= 87%).

For the continuous case with transverse reinforcement, the best model for the FRP contribution seems the CNR-DT200/2004 [43] (MV=1.11, COV=53%) followed by Kotynia [14] (MV=1.02, COV=72%).

In relation to the experimental results for rectangular sections and the side-bonded configuration, for the specimens without transverse reinforcement, the percentage of the contribution of the experimental FRP shear strength in relation to the experimental ultimate strength ranges between 12 and 66 % with a mean value of 45% and a COV of 30%. For the specimens with transverse reinforcement, the percentage of the FRP contribution ranges between 10 and 53% with a mean value of 31% and a COV of 40%. Therefore, the FRP contribution is larger for the cases without transverse reinforcement, as previously observed for other configurations.

Table 7. Statistical results of the experimental to theoretical V_f for rectangular RC beams in a side-bonded configuration w/o and w/ transverse reinforcement ($a/d \geq 2.5$).

There are only 14 tests with a T-section in side-bonded configuration (9 with transverse reinforcement an 5 without transverse reinforcement). The performance of the existing models have not been analysed in these cases due to the small number of tests.

4.4 General performance of the existing theoretical models for the FRP shear strength contribution

Figures 1 to 3 show the performance of the different models when evaluating the FRP shear strength contribution in rectangular RC beams strengthened with different configurations (UD, UC, WD, WC, SD, SC) distinguishing the cases without and with transverse reinforcement. In all plots, the red line indicates an identical value for the experimental and theoretical FRP shear strength contribution. If tests are below the red line, the prediction of the model is conservative. In general, as shown in Figure 1 to 3, the scatter is larger for all the specimens with transverse reinforcement. In relation to the existing models, all of them except the JSCE [51] show conservative predictions for the wrapped configuration despite the internal transverse steel reinforcement ratio. Predictions for the U-shaped configurations seem more accurate, since they are close to 1.0 for many theoretical models, especially for the cases without transverse reinforcement. The fib Bulletin 90 [1], CNR-DT200 R1/2013 [49], fib Bulletin 14 [6], JSCE [51], Pellegrino and Modena [10,18,53], and Chen and Teng [23] predictions seem unconservative for the U-shaped configuration with transverse reinforcement. Mofidi and Chaallal [20] followed by Kotynia [14] are the models that show less scatter for both the U-shaped and side-bonded configurations.

Figures 4 to 6 show the performance of the models, but in this case, for T-sections. A similar trend is observed in all models for T-sections. ACI 440.2R-17 [2] is more conservative for T-sections in all configurations. For the U-shaped configuration with transverse reinforcement, fib Bulletin 14 [6] and JSCE [51] predictions are unconservative. TR-55 is also unconservative but only for the U-shaped continuous case. Since trends are similar to those of rectangular sections, it seems that the shape of the section does not influence very much on the theoretical FRP shear strength contribution.

Figure 1. Experimental vs. theoretical V_f according to Fib Bulletin 90 [1], ACI 440.2R-17 [2], DAfStb [5], CNR-DT-200 R1/2013 [3] and TR-55[4] for rectangular RC beams w/o and with transverse reinforcement for continuous or discnontinous U-shaped, wrapped or side-bonded FRP configurations.

Figure 2. Experimental vs. theoretical V_f according to Fib Bulletin [6], JSCE [51], Rousakis et al. [26], Kotynia [14], and Mofidi and Chaallal [12] for rectangular RC beams w/o and with transverse reinforcement for continuous or discontinuous U-shaped, wrapped or side-bonded FRP configurations.

Figure 3. Experimental vs. theoretical V_f according to Pellegrino and Modena [10,18,53], Monti and Liotta [13], Carolin and Täljsten [42] and Chen and Teng [23], for rectangular RC beams w/o and with transverse reinforcement for continuous or discnontinous U-shaped, wrapped or side-bonded FRP configurations.

Figure 4. Experimental vs. theoretical V_f according to Fib Bulletin 90 [1], ACI 440.2R-17 [2], DAfStb [5], CNR-DT-200 R1/2013 [3] and TR-55[4] for T-RC beams w/o and with transverse reinforcement for continuous or discontinuous U-shaped, wrapped or side-bonded FRP configurations.

Figure 5. Experimental vs. theoretical V_f according to Fib Bulletin 14 [6], JSCE [51], Rousakis et al. [26], Kotynia [14], and Mofidi and Chaallal [12] for T-RC beams w/o and with transverse reinforcement for continuous or discontinuous U-shaped, wrapped or side-bonded FRP configurations.

Figure 6. Experimental vs. theoretical V_f according to Pellegrino and Modena [10,18,53], Monti and Liotta [13], Carolin and Täljsten [42] and Chen and Teng [34], for T-RC beams w/o and with transverse reinforcement for continuous or discontinuous U-shaped, wrapped or side-bonded FRP configurations.

4.4 General performance of the existing theoretical models that predict the ultimate shear strength of FRP-shear strengthened elements

Some of the previous theoretical models give the prediction for the total ultimate shear strength and not only the FRP contribution. When combining a model or formulation that quantifies the FRP shear strength contribution, V_f, with a general model for the calculation of the total shear strength of the beam, the dispersion decreases substantially (for those cases with stirrups or for those w/o stirrups if the concrete contribution is considered) (see Figure 7). This might be explained by the interaction between the different components on the shear strength, that is, by the influence of the FRP in the concrete contribution to the shear strength. In addition, in some cases the contribution of the FRP is less significant than the remaining components (concrete and steel) so the scatter is lower.

Figure 7. Experimental vs. theoretical V_u according to Rousakis et al. [26], Pellegrino and Modena [10,18,53], and Monti and Liotta [13] for rectangular RC beams w/o and with transverse reinforcement for continuous or discontinuous U-shaped, wrapped or side-bonded FRP configurations.

Tables 8 and 9 give the statistical results for some models that predict the total ultimate shear strength (Rousakis et al. [26], Pellegrino and Modena [10,18,53], and Monti and Liotta [13]) for wrapped and U-shaped configurations, respectively. As observed, the model of Monti and Liotta [13] show mean values closer to 1.0. However, the model of Rousakis et al. [26] shows less scatter than the remaining models.

Table 8. Statistical results of the experimental to theoretical of V_u for RC beam with a rectangular section in a wrapped configuration w/o and w/ transverse reinforcement ($a/d \geq 2.5$).

Table 9. Statistical results of the experimental to theoretical of V_u for RC beam with a rectangular section in a U-shaped configuration w/o and w/ transverse reinforcement ($a/d \geq 2.5$).

In general, it is considered that the internal transverse steel reinforcement is yielded at failure. In a real field case, since the FRP strengthening is employed when the unstrengthened element is not able to carry the loads. It is assumed that the internal transverse steel has yielded. However, in a test of an experimental program, the debonding of the FRP external reinforcement might occur before steel yields, as observed in the database. For the 262 tests with stirrups, only 146 out of 262 show a mean value of the tensile stress in the stirrups crossing the shear critical crack higher than its yield strength. This fact should be considered in the theoretical models that assess the total shear strength of FRP shear-strengthened RC elements.

5. ANALYSIS OF THE INFLUENCE OF THE ANGLE OF INCLINATION OF STRUTS IN THE THEORETICAL PREDICTIONS

From the experimental results compiled on the database, some parameters have a significant influence in the calculation of the FRP contribution to the shear strength as observed by Kotynia et al. [50]. In addition, Mofidi and Chaallal [12] identified several major parameters: bond model, effective strain, anchorage length, width-to-spacing ratio for discontinuous configurations, crack angle, crack pattern, effect of transverse steel. Some of them have already been considered in the existing theoretical formulations. However, some of these parameters such as the crack angle, crack pattern or effect of transverse steel are not fully understood and need further research. This section is mainly focused on the study of the influence of the adopted angle of inclination of struts.

The angle of inclination of struts with the beam axis perpendicular to the shear force, θ, should be defined in accordance to the remaining components of the shear strength. In this section, the models of the previous section which do not considered a fixed crack angle have been analysed with different possible definition of the inclination of struts.

As observed in Table 2, some models such that of DAfStb [5], Mofidi and Chaallal [12], Pellegrino and Modena [10,18,53], Monti and Liotta [13], Carolin and Täljsten [42] considered a variable angle θ, in a similar manner than the Eurocode 2 [24].

Kotynia [14] proposes a θ value that depends on the amount of internal transverse reinforcement, which gives values of θ ranging between 35º and 45º.

$$\theta = 35^o \qquad for\ \rho_s < 0.1\% \tag{2}$$

$$\theta = 40^o \qquad for\ 0.1\% \leq \rho_s < 0.2\% \tag{3}$$

$$\theta = 45^o \qquad for\ \rho_s \geq 0.2\% \tag{4}$$

Rousakis et al. [26] considered Marí et al. [56,57] model to calculate the concrete and internal steel contribution to the shear strength. This model defines the θ angle as shown in Eq. (5).

$$cot\theta = \frac{0.85d}{d-x} \leq 2.50 \tag{5}$$

where:

d is the effective depth of the section

x is the neutral axis depth of the cracked section, obtained assuming zero concrete tensile strength.

$$\frac{x}{d} = \alpha_e \rho_l \left(-1 + \sqrt{1 + \frac{2}{\alpha_e \rho_l}}\right) \approx 0.75(\alpha_e \rho_l)^{1/3} \tag{6}$$

where:

α_e is the modular ratio between the longitudinal reinforcement material, E_s, and the secant modulus of the concrete, E_{cm}, $\alpha_e = E_s/E_{cm}$, being ($E_{cm} = 22000(f_{cm}/10)^{0.3} \ngtr 39\ GPa$)

ρ_l is the longitudinal tensile reinforcement ratio referred to the effective depth d and the width b. $\rho_l = A_s/bd$.

As observed, in Eq. (1), since V_f depends on cot θ, as long as the angle decreases the prediction of the FRP contribution increases, and then the model is less conservative.

Figure 8 and 9 show the statistical results in terms of mean value and error, for some of the models included in the previous analysis, with four different possible variable definitions of the θ angle (45º, Kotynia's [14] proposal, Marí et al. proposal [56,57], variable approach of Eurocode 2 [24]). The variable approach of Eurocode 2 [24] is obtained as the optimal angle that equals the shear resistance to the maximum shear force limited by the crushing of the compression struts.

As observed, the scatter of the different models remains almost constant for the different θ definitions. The main difference is related to the mean value, which is less conservative as long as the angle decreases. The θ angle according Kotynia [14] is in between 35 and 45º, the value obtained from Eurocode 2 [24] is around 21º for most cases, and according to variable model of Mari et al. [56,57] ranges from 28 to 41º.

Figure 8. Mean value and dispersion for different θ angles according to different existing models [5], [6], [14], [13], [23] for rectangular RC beams strengthened in a wrapped continuous or discontinuous configuration with and without transverse reinforcement.

Figure 9. Mean value and dispersion for different θ angles according to different existing models [5], [6], [14], [13], [12] [23] for rectangular RC beams strengthened in a wrapped continuous or discontinuous configuration with and without transverse reinforcement.

Figure 10 shows the influence of the θ angle in the different components of the shear strength according the model of Monti and Liotta (2007) [13] for two beams of the database (BS2 from Matthys [58], and T4S2-C45 from Deniaud and Cheng (2003) [59]). As observed in both cases, the FRP and the transverse steel components (V_f and V_s, respectively) decrease when the θ angle increases. Therefore, the predictions are much more conservative with the increment of θ.

Figure 10. Influence of the angle of inclination of struts in the different resisting components according to the formulation of Monti and Liotta (2007) [13] for specimens BS2 (Matthys, 2000 [58]) and T4S2-C45 of Deniaud and Cheng (2003) [59].

7. CONCLUSIONS

A database of 555 tests strengthened in shear by EB FRP sheets was assembled from the existing experimental programs distinguishing between the EB FRP configuration and the existence of internal transverse reinforcement. A comparative analysis of the experimental-to-theoretical ratio of the FRP contribution to the ultimate shear strength has been performed by means of the database. From this analysis, the following conclusions can be drawn:

For rectangular beams without transverse reinforcement strengthened in a wrapped configuration, most of the models show a conservative mean value higher than 2.0 of the experimental-to-theoretical $V_{f,exp}/V_{f,th}$ ratio with COV between 30 and 50%. The fib bulletin 14 [6] shows the best statistical performance for both discontinuous (MV=1.03, COV=37%) and continuous (MV=1.09, COV=27%) configurations.

For rectangular beams with transverse reinforcement strengthened in a wrapped configuration, all models are less conservative, showing the fib bulletin 14 [6] and the modified model of Kotynia [14] the best statistical performance for the discontinuous case (MV=1.04 COV=36%; MV=1.15 COV=38%, respectively), but being unconservative both formulations for the continuous configurations. In this last case the CNR-DT200/2004 [43] shows the best MV=1.00 with a COV=43%.

For T-sections the scatter is larger despite the number of tests is lower. This fact might be explained by the experimental failure mode which is due to the anchor pull out instead of the theoretical failure which is assumed to occur at the bottom corner of the section.

For rectangular beams without transverse reinforcement in a U-shaped configuration, the best statistical performance is given by the fib Bulletin (MV=1.10, COV=39%) for the discontinuous EB FRP and by Mofidi and Chaallal [20] (MV=1.19, COV=28%) for the continuous configuration.

For the same case but with transverse reinforcement, the scatter is larger than for beams without transverse reinforcement. Mofidi and Chaallal [20] show the best statistical performance for both discontinuous (MV=1.17, COV=51%) and continuous cases (MV=1.02, COV=43%).

For T-sections in a U-shaped configuration, the trend of the results is similar to rectangular sections.

For side-bonded FRP configurations, in rectangular beams without transverse reinforcement, the model with best statistical performance is that of Chen and Teng [34] (MV=1.01, COV=46%) for the discontinuous sheets and Kotynia [14] (MV=0.99, COV=56%) for the continuous systems. T-sections were not analysed in this case due to the reduced number of tests.

Results depend mainly on the assumed value for the inclination angle of struts. It has been observed that the models seem more conservative as long as this angle increases up to 45º.

Finally, when predicting the total ultimate shear strength, the performance of the analysed models is better than that obtained when analysing only the FRP shear strength contribution. This might be explained by the importance of the interaction between the different shear strength components. The existence of the FRP might modify the transverse steel contribution. This might justify a modification of the conventional calculation of the experimental FRP shear strength component as the difference between the ultimate shear strength of the strengthened element and the ultimate shear strength of the control specimen.

ACKNOWLEDGEMENTS

This paper has been developed under the framework of the Research Projects "BIA2015-64672-C4-1-R" and "RTI2018-097314-B-C21" funded by the Spanish Ministry of Economy and Competitiveness (MINECO) and co-funded by the European Regional Development Funds (ERDF). The authors would also like to thank the Cost Action TU1207 which funded a short term scientific mission of the first author in Lodz University of Technology.

REFERENCES

[1] fib Task group 5.1. FIB Bulletin 90, Externally applied FRP reinforcement for concrete structures. Lausanne, Switzerland: 2019.

[2] ACI Committee 440. ACI 440.2R-17, Guide for the Design and Construction of Externally Bonded FRP Systems for Strengthening Concrete Structures. Farmington Hills, Michigan, USA: 2017.

[3] Construction C– AC on TR for. CNR-DT 200 R1/2013 Guide for the Design and Construction of Externally Bonded FRP Systems for Strengthening Existing Structures. Rome, Italy: 2013.

[4] 55 CSTR. Design guidance for strengthening concrete structures using fibre composite materials. London, Great Britain: 2012.

[5] German Committee for Reinforced Concrete. DAfStb Heft 595 Erläuterungen und Beispiele zur DAfStb-Richtlinie Verstärken von Betonbauteilen mit geklebter Bewehrung. Berlin, Germany: 2013.

[6] fib Task Group 9.3 FRP Reinforcement for Concrete Structures. Externally bonded FRP reinforcement for RC structures (2001). Technical report on the design and use of externally bonded fibre reinforced polymer reinforcement (FRP EBR) for reinforced concrete structures, Fib Bulletin 14. 2001.

[7] Bousselham A, Chaallal O. Behavior of Reinforced Concrete T-Beams Strengthened in Shear with Carbon Fiber-Reinforced Polymer-An Experimental Study. ACI Struct J 2006;103:339–47.

[8] Bousselham A, Chaallal O. Mechanisms of Shear Resistance of Concrete Beams Strengthened in Shear with Externally Bonded FRP. J Compos Constr 2008;12:499–512. https://doi.org/10.1061/(ASCE)1090-0268(2008)12:5(499).

[9] Chen GM, Teng JG, Chen JF, Rosenboom OA. Interaction between Steel Stirrups and Shear-Strengthening FRP Strips in RC Beams. J Compos Constr 2010;14:498–509. https://doi.org/10.1061/(ASCE)CC.1943-5614.0000120.

[10] Pellegrino C, Modena C. Fiber Reinforced Polymer Shear Strengthening of Reinforced Concrete Beams with Transverse Steel Reinforcement. J Compos Constr 2002;6:104–11. https://doi.org/10.1061/(ASCE)1090-0268(2002)6:2(104).

[11] Pellegrino C, Vasic M. Assessment of design procedures for the use of externally bonded FRP composites in shear strengthening of reinforced concrete beams. Compos Part B Eng 2013;45:727–41. https://doi.org/10.1016/j.compositesb.2012.07.039.

[12] Mofidi A, Chaallal O. Shear strengthening of RC beams with externally bonded FRP composites: Effect of strip-width-to-strip-spacing ratio. J Compos Constr 2011;15:732–42. https://doi.org/10.1061/(ASCE)CC.1943-5614.0000219.

[13] Monti G, Liotta M. Tests and design equations for FRP-strengthening in shear. Constr Build Mater 2007;21:799–809. https://doi.org/10.1016/j.conbuildmat.2006.06.023.

[14] Kotynia R. Shear strengthening of RC beams with polymer composites. Lodz University of Technology, 2011.

[15] Colotti V. Shear interaction effect between transverse reinforcements in FRP-strengthened RC beams. Compos Part B Eng 2013;45:1222–33. https://doi.org/10.1016/j.compositesb.2012.06.009.

[16] Mohamed Ali MS, Oehlers DJ, Seracino R. Vertical shear interaction model between external FRP transverse plates and internal steel stirrups. Eng Struct 2006;28:381–9.

[17] Petrone F, Monti G. FRP-RC Beam in Shear: Mechanical Model and Assessment Procedure for Pseudo-Ductile Behavior. Polymers (Basel) 2014;6:2051. https://doi.org/10.3390/polym6072051.

[18] Pellegrino C, Modena C. An experimentally based analytical model for the shear capacity of FRP-strengthened reinforced concrete beams. Mech Compos Mater 2008;44:231–44. https://doi.org/10.1007/s11029-008-9016-y.

[19] Deniaud C, Cheng JJR. Review of shear design methods for reinforced concrete beams strengthened with fibre reinforced polymer sheets. Can J Civ Eng 2001;28:271–81. https://doi.org/10.1139/cjce-28-2-271.

[20] Mofidi A, Chaallal O. Shear Strengthening of RC Beams with EB FRP: Influencing Factors and Conceptual Debonding Model. J Compos Constr 2011;15:62–74. https://doi.org/10.1061/(ASCE)CC.1943-5614.0000153.

[21] Mofidi A, Chaallal O. Tests and Design Provisions for Reinforced-Concrete Beams Strengthened in Shear Using FRP Sheets and Strips. Int J Concr Struct Mater 2014;8:117–28. https://doi.org/10.1007/s40069-013-0060-1.

[22] Colotti V, Swamy RN. Unified analytical approach for determining shear capacity of RC beams strengthened with FRP. Eng Struct 2011;33:827–42.

[23] Chen JF, Teng JG. Shear capacity of FRP-strengthened RC beams: FRP debonding. Constr. Build. Mater., vol. 17, 2003, p. 27–41.

[24] (CEN) European Committee for Standardization. Eurocode 2: Design of Concrete Structures: Part 1: General Rules and Rules for Buildings. European Committee for Standardization; 2002.

[25] Sas G, Täljsten B, Barros J, Lima J, Carolin A. Are available models reliable for predicting the FRP contribution to the shear resistance of RC beams? J Compos Constr 2009;13:514–34. https://doi.org/10.1061/(ASCE)CC.1943-5614.0000045.

[26] Rousakis TC, Saridaki ME, Mavrothalassitou SA, Hui D. Utilization of hybrid approach towards advanced database of concrete beams strengthened in shear with FRPs. Compos Part B Eng 2016;85:315–35. https://doi.org/10.1016/j.compositesb.2015.09.031.

[27] D’Antino T, Triantafillou TC. Accuracy of design-oriented formulations for evaluating the flexural and shear capacities of FRP-strengthened RC beams. Struct Concr 2016;17:425–42. https://doi.org/10.1002/suco.201500066.

[28] Chaallal O, Nollet M-J, Perraton D. Strengthening of reinforced concrete beams with externally bonded fiber-reinforced-plastic plates: Design guidelines for shear and flexure. Can J Civ Eng 1998;25:692–704.

[29] Triantafillou TC. Shear Strengthening of Reinforced Concrete Beams Using Epoxy-Bonded FRP Composites. ACI Struct J 1998;95:107–15.

[30] Triantafillou TCTC, Antonopoulos CPCP. Design of Concrete Flexural Members Strengthened in

Shear with FRP. vol. 4. 2000. https://doi.org/10.1061/(ASCE)1090-0268(2000)4:4(198).

[31] Khalifa A, Gold WJ, Nanni A, M.I. AA. Contribution of Externally Bonded FRP to Shear Capacity of RC Flexural Members. J Compos Constr 1998;2:195–202.

[32] Khalifa A, Nanni A. Improving shear capacity of existing RC T-section beams using CFRP composites. Cem Concr Compos 2000;22:165–74. https://doi.org/10.1016/S0958-9465(99)00051-7.

[33] Chen JF, Teng JG. Anchorage strength models for FRP and steel plates bonded to concrete. J Struct Eng 2001;127:784–91. https://doi.org/10.1061/(ASCE)0733-9445(2001)127:7(784).

[34] Chen JF, Teng JG. Shear capacity of fiber-reinforced polymer-strengthened reinforced concrete beams: Fiber reinforced polymer rupture. J Struct Eng 2003;129:615–25. https://doi.org/10.1061/(ASCE)0733-9445(2003)129:5(615).

[35] Deniaud C, Cheng JJR. Shear Behavior of Reinforced Concrete T-Beams with Externally Bonded Fiber-Reinforced Polymer Sheets. ACI Struct J 2001;98:386–94.

[36] Deniaud C, Cheng JJR. Simplified shear design method for concrete beams strengthened with fiber reinforced polymer sheets. J Compos Constr 2004;8:425–33. https://doi.org/10.1061/(ASCE)1090-0268(2004)8:5(425).

[37] Adhikary BB, Mutsuyoshi H, Ashraf M. Shear strengthening of reinforced concrete beams using fiber-reinforced polymer sheets with bonded anchorage. ACI Struct J 2004;101:660–8.

[38] Ye, L.P., Lu, X.Z., Chen JF. Design proposals for debonding strengths of FRP strengthened RC beams in the Chinese Design Code. Proc., Int. Symp. Bond Behav. FRP Struct. Int. Inst. FRP Constr. (IIFC), Hong Kong, China., 2005.

[39] Cao SY, Chen JF, Teng JG, Hao Z, Chen J. Debonding in RC beams shear strengthened with complete FRP wraps. J Compos Constr 2005;9:417–28. https://doi.org/10.1061/(ASCE)1090-0268(2005)9:5(417).

[40] Zhang Z, Hsu C-TT. Shear strengthening of reinforced concrete beams using carbon-fiber-reinforced polymer laminates. J Compos Constr 2005;9:158–69. https://doi.org/10.1061/(ASCE)1090-0268(2005)9:2(158).

[41] Carolin A. Carbon fiber reinforced polymers for strengthening of structural elements. Carbon Fibre Reinf Polym Strength Struct Elem 2003.

[42] Carolin A, Täljsten B. Theoretical study of strengthening for increased shear bearing capacity. J

Compos Constr 2005;9:488–96. https://doi.org/10.1061/(ASCE)1090-0268(2005)9:6(488).
[43] CNR (National Research Council) Advisory Committee on technical recommendations for Construction. Guide for the Design and Construction of Externally Bonded FRP Systems for Strengthening Existing Structures. CNR-DT200/. Rome, Italy: 2004.
[44] 440 ACI (ACI) AC. Guide for the design and construction of externally bonded FRP systems for strengthening concrete structures. ACI 440.2R. 2008.
[45] Bukhari IA, Vollum RL, Ahmad S, Sagaseta J. Shear strengthening of reinforced concrete beams with CFRP. Mag Concr Res 2010;62:65–77. https://doi.org/10.1680/macr.2008.62.1.65.
[46] “Building Code Requirements for Structural Concrete (ACI 318-05) and Commentary (318R-05).” Build Code Requir Struct Concr (ACI 318-05) Comment 2005:430.
[47] Fédération Internationale du Béton. fib Model Code for Concrete Structures 2010. vol. 1. Ernst & Sohn; 2013.
[48] Comité Européen de Normalisation (CEN). Eurocode 8. Design of structures for earthquake resistance. Part 3. Assessment and retrofitting of buildings, EN 1998-3. Brussels: 2005.
[49] CNR (National Research Council) Advisory Committee on technical recommendations for construction. Instruzioni per la Progettazione, l’Esecuzione ed il Controllo di Interventi di Conslidamento Statico mediante l’utilizzo di Compositi Fibrorinforzati. CNR-DT200. Rome, Italy: 2013.
[50] Kotynia R, Oller E, Mari AR, Kaszubska M. Efficiency of shear strengthening of RC beams with externally bonded FRP materials – State-of-the-art in the experimental tests. Compos Part B Eng n.d.
[51] JSCE Japanese Society of Civil Engineers. Recommendations for upgrading of concrete structures with use of continuous fiber sheets. 2000.
[52] CIDAR Centre for Infrastructure Diagnosis A and R. Design Guideline for RC structures retrofitted with FRP and metal plates: beams and slabsNo Title. 2006.
[53] Pellegrino C, Modena C. Fiber-reinforced polymer shear strengthening of reinforced concrete beams: Experimental study and analytical modeling. ACI Struct J 2006;103:720–8.
[54] Monti G, Renzelli M, Luciani P. FRP adhesion in uncracked and cracked concrete zones. Proc Sixth Int Symp FRP Reinf Concr Struct 2003:183–92.
[55] Bilotta, A., Ceroni, F., Nigro, E. And Pecce M. Design by testing procedure of debonding load for

RC elements strengthened with EBR FRP materials. In: R. Sen, R. Seracino, C. Shield and W. Gold (eds), Tampa, Florida C, editor. Proc. 10th FRPRCS Int. Symp. ACI SP-275 Fiber-Reinforced Polym. Reinf. Concr. Struct., 2011.

[56] Marí A, Bairán J, Cladera A, Oller E, Ribas C. Shear-flexural strength mechanical model for the design and assessment of reinforced concrete beams. Struct Infrastruct Eng 2015;11:1399–419. https://doi.org/10.1080/15732479.2014.964735.

[57] Cladera A, Marí A, Ribas C, Bairán J, Oller E. Predicting the shear–flexural strength of slender reinforced concrete T and I shaped beams. Eng Struct 2015;101:386–98. https://doi.org/10.1016/j.engstruct.2015.07.025.

[58] Matthys S. Structural behaviour and design of concrete members strengthened with externally bonded FRP reinforcement. University of Ghent, Belgium, 2000.

[59] Deniaud C, Cheng JJR. Reinforced concrete T-beams strengthened in shear with fiber reinforced polymer sheets. J Compos Constr 2003;7:302–10. https://doi.org/10.1061/(ASCE)1090-0268(2003)7:4(302).

[60] Rousakis TC, Saridaki ME, Mavrothalassitou SA, Hui D. Utilization of hybrid approach towards advanced database of concrete beams strengthened in shear with FRPs. Compos Part B Eng 2016;85:315–35. https://doi.org/10.1016/j.compositesb.2015.09.031.

[61] Berset J. Strengthening of reinforced concrete beams with FRP Composites. 1992.

[62] Al-Sulaimani GJ, Sharif A, Basunbul IA, Baluch MH, Ghaleb BN. Shear repair for reinforced concrete by fiberglass plate bonding. ACI Struct J 1994;91:458–64.

[63] Sato Y, Ueda T, Kakuta Y, Tanaka T. Ultimate shear capacity of reinforced concrete beams with carbon fiber sheets. Proc. Third Symp. Non-Metallic Reinf. Concr. Struct., vol. 1, n.d., p. 499–506.

[64] Araki N, Matsuzaki Y, Nakano K, Kataoka T, Fukuyama H. Shear capacity of retrofitted RC members with continuous fiber sheets. Non-Metallic Reinf Concr Struct 1997;1:515–22.

[65] Funakawa I, Shimono K, Watanabe T, Asada S, Ushijima S. Experimental study on shear strengthening with continuous fiber reinforcement sheet and methyl methacrylate resin. Proceeding Third Int. Symp. Non-Metallic Reinf. Concr. Strutures, vol. 1, 1997, p. 491–8.

[66] Kamiharako A, Maruyama K, Takada K, Shimomura T. Evaluation of shear contribution of FRP sheets attached to concrete beams. Nonmet Reinf Concr Struct Proc, 3rd Int Symp 1997;1:467–

74.

[67] Taerwe L, Khalil H, Matthys S. Behaviour of RC beams strengthened in shear by external CFRP sheets. Proc. Third Int. Symp. Non-Metallic Reinf. Concr. Struct., vol. 1, 1997, p. 507–14.

[68] Täljsten B. Strengthening of concrete structures for shear with bonded CFRP-fabrics. Proc US-Canada-Europe Work Bridg Eng 1997:57–64.

[69] Täljsten B, Elfgren L. Strengthening concrete beams for shear using CFRP-materials: evaluation of different application methods. Compos Part B Eng 2000;31:87–96. https://doi.org/10.1016/S1359-8368(99)00077-3.

[70] Umezu K, Fujita M, Nakai H, Tamaki K. Shear behavior of RC beams with aramid fiber sheet. Proc III Int Symp Non Met Reinf Concr Struct 1997;1:491–8.

[71] Sato Y, Ueda T, Kakuta Y, Tanaka T. Shear reinforcing effect of carbon fiber sheet attached to side of reinforced concrete beams. Adv Compos Mater Bridg Struct 1996:621–7.

[72] Khalifa A, Tumialan G, Nanni A, Belarbi A. Shear strengthening of continuous reinforced concrete beams using externally bonded carbon fiber reinforced polymer sheets. Proc. 4th Int. Symp. Fiber Reinf. Polym. Reinf. Reinf. Concr. Struct., 1999, p. 995–1008.

[73] Park SY, Naaman AE, Lopez MM, Till RD. Shear strengthening of RC beams using glued CFRP sheets. FRP Compos Civ Eng 2001;1:669–76.

[74] Li A, Cheikhna Diagana, Delmas Y, Diagana C, Delmas Y. CRFP contribution to shear capacity of strengthened RC beams. Eng Struct 2001;23:1212–20. https://doi.org/10.1016/S0141-0296(01)00035-9.

[75] Khalifa A, Nanni A. Rehabilitation of rectangular simply supported RC beams with shear deficiencies using CFRP composites. Constr Build Mater 2002;16:135–46. https://doi.org/10.1016/S0950-0618(02)00002-8.

[76] Pellegrino C, Modena C. Fiber Reinforced Polymer Shear Strengthening of Reinforced Concrete Beams with Transverse Steel Reinforcement. J Compos Constr 2002;6:104–11. https://doi.org/10.1061/(ASCE)1090-0268(2002)6:2(104).

[77] Moren JE. Shear Behaviour of reinforced concrete deep beams strengthened with CFRP laminates. M.Sc Thesi. 2002.

[78] Beber AJ, Campos Filho A. CFRP composites on shear strengthening of reinforced concrete beams. Ibracon Struct J 2005;1:127–43.

[79] Diagana C, Li A, Gedalia B, Delmas Y. Shear strengthening effectiveness with CFF strips. Eng Struct 2003;25:507–16. https://doi.org/10.1016/S0141-0296(02)00208-0.

[80] Täljsten B. Strengthening concrete beams for shear with CFRP sheets. Constr Build Mater 2003;17:15–26. https://doi.org/10.1016/S0950-0618(02)00088-0.

[81] Wong RSY, Vecchio FJ, Vecchio RSYW and FJ. Towards modeling of reinforced concrete members with externally bonded fiber-reinforced polymer composites. ACI Struct J 2003;100:47–55. https://doi.org/10.14359/12438.

[82] Abdel-Jaber MS, Walker PR, Hutchinson AR. Carbon fiber-reinforced polymer plates as shear strengthening for beams. Mater Struct 2003;36:291–301.

[83] Zhang Z, Hsu C-TT, Moren J. Shear strengthening of reinforced concrete deep beams using carbon fiber reinforced polymer laminates. J Compos Constr 2004;8:403–14. https://doi.org/10.1061/(ASCE)1090-0268(2004)8:5(403).

[84] Allam S, Ebeido T. Retrofitting of RC beams predamaged in shear using CFRP sheets 2003;42.

[85] Adhikary BB, Mutsuyoshi H. Behavior of concrete beams strengthened in shear with carbon-fiber sheets. J Compos Constr 2004;8:258–64. https://doi.org/10.1061/(ASCE)1090-0268(2004)8:3(258).

[86] Song FX, Fan CZ, Jie L. Experimental research on shear strengthening of reinforde concrete beams with externally bonded CFRP sheets. Southeast University NanJing, China.; 2004.

[87] Ianniruberto U, Imbimbo M. Role of fiber reinforced plastic sheets in shear response of reinforced concrete beams: Experimental and analytical results. J Compos Constr 2004;8:415–24. https://doi.org/10.1061/(ASCE)1090-0268(2004)8:5(415).

[88] Miyajima H, Kosa K, Tasaki K, Matsumoto S. Shear strengthening of RC beams using carbon fiber sheets & its resistance mechanism. Proc. Fifth Work. Saf. Stab. Infrastructures against Environ. Impacts, 2005, p. 114–25.

[89] Qu Z, Lu X. Size effect of shear contribution of externally bonded FRP U-jackets for RC beams. Proc. Int. Symp. Bond Behav. FRP Struct. (BBFS 2005), 2005, p. 371–80.

[90] Saafan MAA. Shear Strengthening of Reinforced concrete beams using GFRP wraps. Acta Polytech 2006;46:24–32.

[91] Rizzo A, De Lorenzis L. Behavior and capacity of RC beams strengthened in shear with NSM FRP reinforcement. Constr Build Mater 2009;23:1555–67.

https://doi.org/10.1016/j.conbuildmat.2007.08.014.

[92] Barros JAOO, Dias SJEE. Near surface mounted CFRP laminates for shear strengthening of concrete beams. Cem Concr Compos 2006;28:276–92. https://doi.org/10.1016/j.cemconcomp.2005.11.003.

[93] Norris T, Saadatmanesh H, Ehsani MR. Shear and flexural strengthening of R/C beams with carbon fiber sheets. J Struct Eng 1997;123:903–11. https://doi.org/10.1061/(ASCE)0733-9445(1997)123:7(903).

[94] Grande E, Imbimbo M, Rasulo A. Effect of transverse steel on the response of RC beams strengthened in shear by FRP: Experimental study. J Compos Constr 2009;13:405–14. https://doi.org/10.1061/(ASCE)1090-0268(2009)13:5(405).

[95] Zhang G, Kishi N, Mikami H. Effects of Bonding Configurations on Shear Behavior of RC Beams Reinforced With Aramid FRP Sheets. In: Patras U of, editor. Int. 8thStructures, Symp. Fiber-Reinforced Polym. Reinf. Concr., Greece: 2007.

[96] Mosallam AS, Banerjee S. Shear enhancement of reinforced concrete beams strengthened with FRP composite laminates. Compos Part B Eng 2007;38:781–93. https://doi.org/10.1016/j.compositesb.2006.10.002.

[97] Jayaprakash J, Abdul Samad AA, Anvar Abbasovich A, Abang Ali AA. Shear capacity of precracked and non-precracked reinforced concrete shear beams with externally bonded bi-directional CFRP strips. Constr Build Mater 2008;22:1148–65. https://doi.org/10.1016/j.conbuildmat.2007.02.008.

[98] Godat A, Qu Z, Lu XZ, Labossìre P, Ye LP, Neale KW. Size effects for reinforced concrete beams strengthened in shear with CFRP strips. J Compos Constr 2010;14:260–71. https://doi.org/10.1061/(ASCE)CC.1943-5614.0000072.

[99] Murat Tanarslan H. Repairing & Strengthening Earthquake Damaged RC Beams with Composites. World Acad Sci Eng Technol 2013;7:1360–4.

[100] Alzate A, Arteaga A, De Diego A, Cisneros D, Perera R. Shear strengthening of reinforced concrete members with CFRP sheets [Refuerzo externo a cortante con láminas de CFRP en elementos de hormigón armado]. Mater Constr 2013;63:251–65. https://doi.org/10.3989/mc.2012.06611.

[101] Leung CKY, Chen Z, Lee S, Ng M, Xu M, Tang J. Effect of size on the failure of geometrically

similar concrete beams strengthened in shear with FRP strips. J Compos Constr 2007;11:487–96. https://doi.org/10.1061/(ASCE)1090-0268(2007)11:5(487).

[102] Khan AR, Ayub T. Performance of RC beams strengthened in shear by externally bonded U-shaped wraps. SBEIDCO – 1st Int. Conf. Sustain. Built Environ. Infrastructures Dev. Ctries. ENSET Oran, 2009, p. 151–8.

[103] Kim G, Sim J, Oh H. Shear strength of strengthened RC beams with FRPs in shear. Constr Build Mater 2008;22:1261–70. https://doi.org/10.1016/j.conbuildmat.2007.01.021.

[104] Bae S-WS-W, Belarbi A. Behavior of Various Anchorage Systems Used for Shear Strengthening of Concrete Structures with Externally Bonded FRP Sheets. J Bridg Eng 2013;18:837–47. https://doi.org/10.1061/(ASCE)BE.1943-5592.0000420.

[105] Chajes MJ, Januszka TF, Mertz DR, Thomson Jr. TA, Finch Jr. WW. Shear strengthening of reinforced concrete beams using externally applied composite fabrics. ACI Struct J 1995;92:295–303.

[106] Khalifa A, Nanni A. Improving shear capacity of existing RC T-section beams using CFRP composites. Cem Concr Compos 2000;22:165–74. https://doi.org/10.1016/S0958-9465(99)00051-7.

[107] Deniaud C, Cheng JJR. Shear behavior of RC T-beams with externally bonded FRP sheets. ACI Struct J 2000.

[108] Annaiah R. Shear performance of RC beams strengthened in situ with composites / 2020.

[109] Chaallal O, Shahawy M, Hassan M. Performance of Reinforced Concrete T-Girders Strengthened in Shear with Carbon Fiber-Reinforced Polymer Fabric. ACI Struct J 2002;99:335–43.

[110] Bousselham A, Chaalal O, Chaallal O. Effect of transverse steel and shear span on the performance of RC beams strengthened in shear with CFRP. Compos Part B Eng 2006;37:37–46. https://doi.org/10.1016/j.compositesb.2005.05.012.

[111] Gamino AL, Sousa J, Manzoli OL, Bittencourt TN. R/C Structures strengthened with CFRP Part II: Analysis of shear models. Rev IBRACON Estruturas e Mater 2010;3:24–49.

[112] Dias SJE, Barros JAO. Shear strengthening of RC T-section beams with low strength concrete using NSM CFRP laminates. Cem Concr Compos 2011;33:334–45. https://doi.org/10.1016/j.cemconcomp.2010.10.002.

[113] Oller E, Pujol M, Marí A. Contribution of externally bonded FRP shear reinforcement to the

shear strength of RC beams. Compos Part B Eng 2019;164:235–48. https://doi.org/https://doi.org/10.1016/j.compositesb.2018.11.065.

[114] Czaderski C. Shear strengthening with prefabricated CFRP L-shaped plates. 1st Fib Conf., vol. 86, 2002, p. 299–308. https://doi.org/10.2749/222137802796336757.

[115] Koutas L, Triantafillou TC. Use of anchors in shear strengthening of reinforced concrete T-beams with FRP. J Compos Constr 2013;17:101–7. https://doi.org/10.1061/(ASCE)CC.1943-5614.0000316.

[116] El-Saikaly G, Godat A, Chaallal O. New Anchorage Technique for FRP Shear-Strengthened RC T-Beams Using CFRP Rope. J Compos Constr 2015;19:4014064. https://doi.org/10.1061/(ASCE)CC.1943-5614.0000530.

[117] Kim Y, Ghannoum WM, Jirsa JO. Shear behavior of full-scale reinforced concrete T-beams strengthened with CFRP strips and anchors. Constr Build Mater 2015;94:1–9. https://doi.org/10.1016/j.conbuildmat.2015.06.005.

[118] Ozden S, Atalay HM, Akpinar E, Erdogan H, Vulaş YZ. Shear strengthening of reinforced concrete T-beams with fully or partially bonded fibre-reinforced polymer composites. Struct Concr 2014;15:229–39. https://doi.org/10.1002/suco.201300031.

[119] Panda KC, Bhattacharyya SK, Barai S V. Shear strengthening of RC T-beams with externally side bonded GFRP sheet. J Reinf Plast Compos 2011;30:1139–54. https://doi.org/10.1177/0731684411417202.

[120] Panda KC, Bhattacharyya SK, Barai S V. Effect of transverse steel on the performance of RC T-beams strengthened in shear zone with GFRP sheet. Constr Build Mater 2013;41:79–90. https://doi.org/10.1016/j.conbuildmat.2012.11.098.

[121] Panigrahi SK, Deb A, Bhattacharyya SK. Modes of failure in shear deficient RC T-beams strengthened with FRP. J Compos Constr 2016;20:04015029. https://doi.org/10.1061/(ASCE)CC.1943-5614.0000586.

[122] Randl N, Harsányi P. Developing optimized strengthening systems for shear-deficient concrete members. Struct Concr 2018;19:116–28. https://doi.org/10.1002/suco.201600187.

[123] Belarbi A, Bae SW, Brancaccio A. Behavior of full-scale RC T-beams strengthened in shear with externally bonded FRP sheets. Constr Build Mater 2012;32:27–40.

[124] Sang-Wook B, Abdeldjelil B. Behavior of Various Anchorage Systems Used for Shear

Strengthening of Concrete Structures with Externally Bonded FRP Sheets. J Bridg Eng 2013;18:837–47. https://doi.org/10.1061/(ASCE)BE.1943-5592.0000420.

[125] Altin S, Anil Ö, Kopraman Y, Mertoğlu Ç, Kara ME. Improving shear capacity and ductility of shear-deficient RC beams using CFRP strips. J Reinf Plast Compos 2010;29:2975–91. https://doi.org/10.1177/0731684410363182.

[126] Chen GM, Zhang Z, Li YL, Li XQ, Zhou CY. T-section RC beams shear-strengthened with anchored CFRP U-strips. Compos Struct 2016;144:57–79. https://doi.org/https://doi.org/10.1016/j.compstruct.2016.02.033.

[127] Yungon Kim Wassim M. Ghannoum, and James O. Jirsa KQ, Kim Y, Quinn K, Ghannoum WM, Jirsa JO. Strengthening of Reinforced Concrete T-Beams Using Anchored CFRP Materials. ACI Struct J 2014;111:1027–36. https://doi.org/10.14359/51687025.

[128] Simon Bourget and Omar Chaallal GE-S. Behavior of Reinforced Concrete T-Beams Strengthened in Shear Using Closed Carbon Fiber-Reinforced Polymer Stirrups Made of Laminates and Ropes. ACI Struct J n.d.;114. https://doi.org/10.14359/51700786.

[129] Mofidi A, Thivierge S, Chaallal O, Shao Y. Behavior of reinforced concrete beams strengthened in shear using L-shaped CFRP plates: Experimental investigation. J Compos Constr 2014;18. https://doi.org/10.1061/(ASCE)CC.1943-5614.0000398.

[130] Tamer E-M, Yousef C, El-Maaddawy T, Chekfeh Y. Retrofitting of Severely Shear-Damaged Concrete T-Beams Using Externally Bonded Composites and Mechanical End Anchorage. J Compos Constr 2012;16:693–704. https://doi.org/10.1061/(ASCE)CC.1943-5614.0000299.

[131] Frederick F, Sharma UK, Gupta VK. Influence of End Anchorage on Shear Strengthening of Reinforced Concrete Beams Using CFRP Composites. Curr Sci 2017;112:973–81. https://doi.org/10.18520/cs/v112/i05/973-981.

[132] Chaallal O, Mofidi A, Benmokrane B, Neale K. Embedded through-section FRP rod method for shear strengthening of RC beams: Performance and comparison with existing techniques. J Compos Constr 2011;15:374–83. https://doi.org/10.1061/(ASCE)CC.1943-5614.0000174.

APPENDIX 1. Summary of existing equations to evaluate the total shear strength or the FRP contribution to the total shear strength. Units are in SI (N, mm)

fib Buletin 90[1]

$V_{Rd} = V_{Rd,s} + V_{Rd,f} + V_{ccd} + V_{td}$

$V_{Rd,f} = \frac{A_{fw}}{s_f} h_f f_{fwd}(cot\theta + cot\alpha_f)sin\alpha_f$

$\frac{A_{fw}}{s_f}$ for bonded strips: $2 \cdot t_f \, w_f / s_f$
for continuous bonded reinforcement: $2 \cdot t_f \sin\alpha_f$

f_{fwd}

Closed FRP $f_{fwd} = f_{fwd,c} = k_R \alpha_c f_{fd}$

k_R $k_R = \begin{cases} 0.5\frac{r_c}{50}\left(2 - \frac{r_c}{50}\right) & r_c < 50\ mm \\ 0.5 & r_c \geq 50\ mm \end{cases}$

r_c radius at the corners of the cross section

a_t creep factor of 0.80

f_{fd} ultimate strength of the FRP reinforcement

U-shaped configuration $f_{fwd} = min(f_{fbwd}, f_{fwd,c})$

for bonded strips:

$for\ h_f/sin\alpha_f \geq l_e\ and\ l_e \leq s_f/(cot\theta + cot\alpha_f)sin\alpha_f \leq h_f/sin\alpha_f:\ f_{fbwd} = \frac{f_{bk}}{\gamma_{fb}}$

$for\ h_f/sin\alpha_f \geq l_e\ and\ s_f/(cot\theta + cot\alpha_f)sin\alpha_f \leq l_e: f_{fbwd} = \left[1 - \left(1 - \frac{2}{3}\frac{ms_f}{l_e}\right)\frac{m}{n}\right]\frac{f_{bk}}{\gamma_{fb}}$

$for\ h_f/sin\alpha_f \leq l_e\ and\ s_f/(cot\theta + cot\alpha_f)sin\alpha_f \leq h_f/sin\alpha_f: f_{fbwd} = \frac{2}{3}\frac{(ns_f)/[(cot\theta + cot\alpha_f)sin\alpha_f]}{l_e}\frac{f_{bk}}{\gamma_{fb}}$

n number of strips crossed by shear crack: integer quotient $h_f\ (cot\theta + cot\alpha_f)/s_f$

m number of strips for which the bond length is less than l_e: $l_e\ (cot\theta + cot\alpha_f)sin\alpha_f/s_f$

l_e maximum bond length: $l_{b,max} = \frac{\pi}{2}\sqrt{\frac{E_f t_f s_{0k}}{\tau_{b1}}}$

f_{fbk} bond strength $f_{fbk} = \begin{cases} \sqrt{\frac{E_f s_{0k} \tau_{b1k}}{t_f}}\frac{s_r}{l_e}\left(2 - \frac{s_r}{l_e}\right) & for\ \ s_r < l_e \\ \sqrt{\frac{E_f s_{0k} \tau_{b1k}}{t_f}} & for\ \ s_r \geq l_e \end{cases}$

τ_{b1k} characteristic value of maximum bond stress
CFRP strips: $\tau_{b1k} = 0.37\sqrt{f_{cm}f_{ctm}}$
$\tau_{b1m} = 0.53\sqrt{f_{cm}f_{ctm}}$
CFRP sheets: $\tau_{b1k} = 0.44\sqrt{f_{cm}f_{ctm}}$
$\tau_{b1m} = 0.72\sqrt{f_{cm}f_{ctm}}$

s_{0k} characteristic value of maximum bond slip
CFRP strips: 0.20 mm (mean value 0.21 mm)
CFRP sheets: 0.23 mm (mean value 0.24 mm)

κ_b 1.128

for full area bond:

$for\ h_f/sin\alpha_f \geq l_e: f_{fbwd} = \left[1 - \frac{1}{3}\frac{l_e}{(h_f/sin\alpha_f)}\right]\frac{f_{bk}}{\gamma_{fb}}$

$for\ h_f/sin\alpha_f \le l_e$: $f_{fbwd} = \frac{2}{3}\frac{h_f/sin\alpha_f}{l_e}\frac{f_{bk}}{\gamma_{fb}}$

CNR DT-200 R1/2013 [3]

$V_{Rd} = min\{V_{Rd,s} + V_{Rd,f}, V_{Rd,max}\}$

$V_{Rd,s}$ steel contribution to the shear capacity according to the current building code

$V_{Rd,max}$ ultimate strength of the concrete strut to be evaluated according to the current building code

U-shaped or wrapped: $V_{Rd,f} = \frac{1}{\gamma_{Rd}} 0.9 d f_{fed} 2 t_f (cot\theta + cot\beta)\frac{w_f}{s_f}$

γ_{Rd} partial safety factor 1.20

θ angle of shear cracks to be assumed equal to 45º unless a more detailed calculation is made

w_f, s_f FRP width and spacing measured orthogonally to fibre direction. For continuous FRP, $\frac{w_f}{s_f} = 1.0$

f_{fed} Effective FRP design strength

U-shaped: $f_{fed} = f_{fdd}\left[1 - \frac{1}{3}\frac{l_e sin\beta}{min\{0.9d, h_w\}}\right]$

f_{fdd}: $f_{fdd} = \frac{1}{\gamma_{f,d}}\sqrt{\frac{2E_f\Gamma_{Fd}}{t_f}}$

Γ_{Fk}: $\Gamma_{Fd} = \frac{k_b k_G}{FC}\sqrt{f_{cm}f_{ctm}}$

k_b: $k_b = \sqrt{\frac{2-\frac{b_f}{b}}{1+\frac{b_f}{b}}} \ge 1.0$ where $\frac{b_f}{b} \ge 0.25$

k_G: *k_G = 0.023 mm or 0.0037 mm for pre-cured or wet lay-up*

l_e: $l_e = max\left\{\frac{1}{\gamma_{Rd}f_{bd}}\sqrt{\frac{\pi^2 E_f t_f \Gamma_{Fd}}{2}}, 200mm\right\}$

Wrapped: $f_{fed} = f_{fdd}\left[1 - \frac{1}{6}\frac{l_e sin\beta}{min\{0.9d, h_w\}}\right] + \frac{1}{2}(\phi_R f_{fd} - f_{fdd})\left[1 - \frac{l_e sin\beta}{min\{0.9d, h_w\}}\right]$

$\phi_R = 0.2 + 1.6\frac{r_c}{b_w}$ $\quad 0 \le \frac{r_c}{b_w} \le 0.5$

r_c corner radius of the section

DAfStb [5]

$V_{Rd} = V_{Rd,s} + V_{Rd,f} + V_{ccd} + V_{td}$

$V_{Rd,f} = \frac{A_{fw}}{s_f} d_f f_{fwd}(cot\theta + cot\alpha_f)sin\alpha_f$

$\frac{A_{fw}}{s_f}$ for bonded strips: $2 \cdot t_f\, w_f / s_f$

for continuous bonded reinforcement: $2 \cdot t_f sin\alpha_f$

f_{fwd}

Closed FRP: $f_{fwd} = f_{fwd,c} = k_R \alpha_c f_{fd}$

k_R: $k_R = \begin{cases} 0.5\frac{r_c}{60}\left(2 - \frac{r_c}{60}\right) & r_c < 60\ mm \\ 0.5 & r_c \ge 60\ mm \end{cases}$

r_c radius at the corners of the cross section

α_c creep factor of 0.75

f_{fd} ultimate strength of the FRP reinforcement

U-shaped configuration $f_{fwd} = min(f_{bfwd}, f_{fwd,c})$

for bonded strips:

$for\ \ d_f \ge l_{b,max}\ and\ l_{b,max} \le s_f \le d_f:\ f_{bfwd} = \frac{f_{bk,max}}{\gamma_{fb}}$

$for\ \ d_f \ge l_{b,max}\ and\ s_f \le l_{b,max}: f_{bfwd} = \frac{f_{bk,max}}{\gamma_{fb}}\left\{\left[1 - \frac{(m-1)}{(n-1)}\right] + \frac{m(m-1)s_f}{2(n-1)l_{b,max}}\right\}$

$for\ \ d_f \le l_{b,max}\ \ and\ \ s_f \le d_f:\ f_{bfwd} = \frac{f_{bk,max}}{\gamma_{fb}}\frac{ns_f}{2l_{b,max}}$

n number of strips crossed by shear crack

m number of strips for which the bond length is less than $l_{b,max}$

$l_{b,max}$	maximum bond length	$$l_{b,max} = \frac{2}{\kappa_b}\sqrt{\frac{E_f t_f s_{f0k}}{\tau_{f1k}}}$$
$f_{bk,max}$	bond strength	$$f_{bk,max} = \sqrt{\frac{E_f s_{f0k}\tau_{f1k}}{t_f}}$$
τ_{f1k}	characteristic value of maximum bond stress	$$\tau_{f1k} = 0.311\sqrt{f_{cm}f_{ctm,surf}}$$
s_{f0k}	characteristic value of maximum bond slip	0.201 mm
κ_b	1.128	
$f_{ctm,surf}$	mean axial tensile surface strength of concrete	

TR-55 [4]

$$V_{Rd} = V_{Rd,s} + V_{Rd,f}$$

$$V_{Rd,s} = \frac{A_{sw}}{s} z f_{ywd} cot\theta$$

$\frac{A_{sw}}{s}$ cross sectional area of steel shear reinforcement/longitudinal spacing of steel shear stirrups

z lever arm between the longitudinal steel reinforcement and the centroid of the compression section

f_{ywd} design yield strength of the steel shear reinforcement

θ angle between the concrete compression and the beam axis perpendicular to the shear force

$$V_{Rd,f} = \frac{A_{fw}}{s_f}\left(d_f - \frac{n_s}{3} l_{t,max} cos\alpha_f\right) E_{fd}\varepsilon_{fse}\left(sin\alpha_f + cos\alpha_f\right)$$

$\frac{A_{fw}}{s_f}$ area of FRP ($2 \cdot b_f \cdot t_f$) measured perpendicular to the direction of the fibres/longitudinal spacing of the FRP. For continuous FRP sheet, s_f is taken as 1.0.

- b_f width of the FRP laminate measured perpendicular to the direction of the fibres. For continuous FRP sheet, b_f is taken as $\cos\alpha_f$
- t_f thickness of the FRP laminate

d_f effective depth of the FRP strengthening, measured from the top to the FRP shear strengthening to the steel tension reinforcement

n_s 0 for a fully wrapped beam; 1.0 when FRP is bonded continuously to the sides and bottom of a beam (U-shaped) and 2.0 when it is bonded to only the sides of a beam

$l_{t,max}$ anchorage length required to develop full anchorage capacity

$$l_{t,max} = 0.7\sqrt{\left(E_{fd}t_f/f_{ctk}\right)}$$

E_{fd} design tensile modulus of the FRP laminate

ε_{fse} effective strain in the FRP for shear strengthening

$$\varepsilon_{fse} = min\left(\frac{\varepsilon_{fd}}{2}; 0.5\sqrt{\frac{f_{ctk}}{E_{fd}t_f}}; 0.004\right)$$

- ε_{fd} design ultimate strain capacity of FRP
- f_{ctk} characteristic tensile strength of the concrete

α_f angle between the principal fibres of the FRP and a line perpendicular to the longitudinal axis of the member. α_f is positive when the principal fibres of FRP are rotated away from the direction in which a shear crack will form.

ACI-440.2R-17 [2]

$\phi V_n = \phi_f \left(V_c + V_s + \psi_f V_f \right) \geq V_u$

ϕ strength reduction factor, $\phi = 0.85$

ψ_f additional FRP strength reduction factor, $\psi_f = 0.95$ for wrapped, $\psi_f = 0.85$ for U-shaped or side-bonded

V_c, V_s nominal shear strength of concrete and steel

V_u factored required shear strength

$V_f = \dfrac{A_f E_f \varepsilon_{fe} \left(sin\alpha_f + cos\alpha_f \right) d_f}{s_f}$ nominal shear strength of FRP

A_f area of FRP shear reinforcement $A_f = 2nt_f w_f$

ε_{fe} effective strain in FRP laminates $\varepsilon_{fe} = 0.004 \leq 0.75\varepsilon_{fu}$ for wrapped

$\varepsilon_{fe} = k_v \quad {}_{fu} \leq 0.004$ for U-shaped or side-bonded

ε_{fu} $\varepsilon_{fu} = C_E \varepsilon_{fu}^*$

C_E environmental reduction factor

ε_{fu}^* ultimate rupture strain of FRP reinforcement

k_v bond reduction coeff. $k_v = \dfrac{k_1 k_2 L_e}{11900\varepsilon_{fu}} \leq 0.75$

L_e active bond length $L_e = \dfrac{23300}{\left(n_f t_f E_f \right)^{0.58}}$

k_1 factor $k_1 = \left(\dfrac{f_{ck}}{27} \right)^{2/3}$

k_2 factor $k_2 = \begin{cases} \dfrac{d_f - L_e}{d_f} & for\ U - jacketing\ (U) \\ \dfrac{d_f - 2L_e}{d_f} & for\ side\ bonding\ (S) \end{cases}$

d_f effective depth of the FRP shear reinforcement

α_f angle of the FRP shear reinforcement with the longitudinal axis of the beam

$V_s + V_f \leq 8\sqrt{f_{ck}} b_w d$

---

fib Bulletin 14 [6]

$V_{Rd} = min\{ V_{cd} + V_{sd} + V_{fd}, V_{Rd2} \}$ (EC2 Format)

$V_{fd} = 0.9\varepsilon_{fd,e} E_f \rho_f b_w d (cot\theta + cot\alpha) sin\alpha$

$\varepsilon_{fd,e}$ design value of the effective strain

$\varepsilon_{fd,e} = \varepsilon_{fk,e} / \gamma_f$

$\varepsilon_{fk,e}$ characteristic value of the effective strain

$\varepsilon_{fk,e} = k\varepsilon_{f,e}$ where $k = 0.8$

$\varepsilon_{f,e}$ fully wrapped (or properly anchored CFRP-FRP fracture controls

$$\varepsilon_{f,e} = 0.17 \left(\frac{{f_{cm}}^{2/3}}{E_f \rho_f} \right)^{0.30} \varepsilon_{fu}$$

side or U-shaped CFRP jackets

$$\varepsilon_{f,e} = min \left[0.65 \left(\frac{{f_{cm}}^{2/3}}{E_f \rho_f} \right)^{0.56} 10^{-3}, 0.17 \left(\frac{{f_{cm}}^{2/3}}{E_f \rho_f} \right)^{0.30} \varepsilon_{fu} \right]$$

fully wrapped AFRP-FRP fracture controls

$$\varepsilon_{f,e} = 0.048\left(\frac{f_{cm}{}^{2/3}}{E_f\rho_f}\right)^{0.47} \varepsilon_{fu}$$

ρ_f — FRP reinforcement ratio equal to $2t_f sin\alpha/b_w$ for continuously bonded shear reinforcement of thickness t_f, or $(2t_f/b_w)(w_f/s_f)$

E_f — elastic modulus of FRP in the principal fibre orientation in GPa

θ — angle of diagonal crack with respect to the member axis, assumed equal to 45º

JSCE [51]

$V_{fd} = \frac{1}{\gamma_f}A_f\varepsilon_{fe}E_f z\frac{(sin\alpha+cos\alpha)}{s_f}$

ε_{fe} — $\varepsilon_{fe} = K\varepsilon_{fud}$

K — $K = 1.68 - 0.67R$ $\quad 0.4 \le K \le 0.8$

R — $R = (\rho_f E_f)^{1/4}\varepsilon_{fud}^{2/3}\left(\frac{1}{f_{cd}}\right)^{1/3}$ $\quad 0.5 \le R \le 2.0$

$\varepsilon_{fud} = \frac{f_{fu}}{E_f\lambda_f}$ $\quad \lambda_f = 1.25$

Rousakis et al. [60]

$V_{Rd} = V_{cd} + V_{sd} + V_{fd}$

$V_{fd} = 0.9\varepsilon_{fd,e}E_f\rho_f b_w d(cot\theta + cot\alpha)sin\alpha$ (Fib Bulletin 14, 2001)

$f_{f,e,impr}$ —

$$f_{f,e,impr} = 0.0103 f_{f,m0}\left(\frac{f_{f,e}}{f_{f,m0}}\right)^{1.5297}$$

$$f_{f,m0} = 1\ MPa$$

$f_{f,e}$is the FRP stress at failure of different recommendations. According to Rousakis et al. (2016), best results were obtained for fib Bulletin 14 (2001)

V_{cd}, V_{sd} — Concrete and transverse steel contribution obtained according to Marí et al. (2014) assuming θ=45º.

Mofidi and Chaallal [20]

$V_f = \rho_f E_f \varepsilon_{fe} b d_f(cot\theta + cot\alpha_f)sin\alpha_f$

(Proposed model not valid for fully wrapped configurations)

ρ_f — $\rho_f = \frac{2t_f w_f}{b s_f}$. For a continuous FRP sheet, w_f and s_f can be assumed equal to 1.0. For a strip configuration, the effective width is the sum of the FRP strip widths within the effective width zone.

E_f — elastic modulus of the FRP in the principal fibre-orientation direction

ε_{fe} — effective strain of FRP

$$\varepsilon_{fe} = 0.31\beta_c\beta_l\beta_w\sqrt{\frac{\sqrt{f_c}}{t_f E_f}}$$

β_c — cracking modification factor based on the rigidity of FRP and transverse steel

$$\beta_c = \begin{cases} \dfrac{0.6}{\sqrt{\rho_f E_f + \rho_s E_s}} & for\ U-shaped \\ \dfrac{0.6}{\sqrt{\rho_f E_f + \rho_s E_s}} & for\ side-bonded \end{cases}$$

ρ_s — transverse steel ratio. $\rho_s = A_{st}/(s b_w)$

E_s — elastic modulus transverse steel

	β_l	coefficient to compensate for insufficient anchorage length	$\beta_l = \begin{cases} 1 & if\ \ L_{max}/L_e \geq 1 \\ (2 - L_{max}/L_e)\, L_{max}/L_e & if\ \ L_{max}/L_e < 1 \end{cases}$
		L_{max}	$L_{max} = \begin{cases} d_f/sin\alpha_f & for\ U - shaped \\ d_f/2sin\alpha_f & for\ side - bonded \end{cases}$
		L_e	$L_e = \sqrt{\dfrac{E_f t_f}{2f_{ct}}}$
	β_w	FRP-width to spacing ratio coefficient	$\beta_w = \sqrt{\dfrac{2 - w_f/s_f}{1 + w_f/s_f}}$
b	width of the concrete beam cross-section		
d_f	distance from the extreme compression fibre to the centroid of the tension reinforcement		
θ	angle of concrete shear crack		
α_f	angle of inclination of FRP fibres		

Kotynia [14]

V_f

U-shaped or side-bonded $V_f = 2\sum_{i=1}^{nf_{min}} P_i sin\alpha$

P_i transferred force between each EB FRP strip and the concrete

$$P_i = \beta_1 b_f \sqrt{2G_f k_E E_f t_f}$$

$$\beta_1 = \begin{cases} 1 & for\ L_i > L_e \\ sin\left(\dfrac{\pi L_i}{2L_e}\right) & for\ L_i \leq L_e \end{cases}$$

n_{fmin} number of FRP strips crossing the critical shear crack

$$n_{fmin} = \frac{h_{net}}{s_f}\left(cot\theta + cot\alpha_f\right)$$

h_{net} bonded height of the FRP in the direction perpendicular to longitudinal axis of the beam

G_f fracture energy which depends on the bond model. In this case the model of Bilotta et al. (2011) has been adopted with: $G_f = 0.25^2 k_b^2 f_{cm}^{2/3}$, where k_b is a shape factor given by: $k_b = \sqrt{\frac{2-b_f/b}{1+b_f/b}}$, where b corresponds to s_f projected in the direction perpendicular to the FRP fibres

L_i bonded length of each FRP sheet

L_e effective bonded length of the FRP which also depends on the bond model, $L_e = \frac{\pi}{2}\sqrt{\frac{E_f t_f s_0}{\tau_{b1}}}$ where according to Bilotta et al. (2011); $\tau_{b1} = 0.50 k_b^2 f_{cm}^{2/3}$ and $s_0 = 0.25$ mm

k_E reduction factor for the FRP modulus of elasticity when the tensile force acting on it is not in the same direction as the fibres (γ angle)

$$k_E = \frac{1}{cos^4\gamma + k_1 sin^4\gamma + (k_2 - 2\nu)cos^2\theta sin^2\theta}$$

k_1, k_2	factors which considers the relationship between the elastic modulus in the direction of the fibres and perpendicular to them (k_1) and the relationship between the elastic modulus in the direction of the fibres and the shear modulus (k_2).

For the discontinuous configuration, when calculating the bonded length L_i of the different strips, if we don't know the exact position of the strips, only its width and spacing, several assumptions can be analyzed such as z_1=0, z_2=0 or $z_1 = z_2$. The minimum V_f value between all these assumptions will be considered in the calculations.

$$z_1 = z_2 = \frac{h_{net}\left(cot\theta + cot\alpha_f\right) - n_{fmin}s_f}{2}$$

$$L_0 = z_1 \frac{sin\theta}{sin\left(\alpha_f + \theta\right)}$$

$$L_{imin} = min\begin{cases} L_{ai} = L_0 + iL_s \\ L_{bi} = L_f - (L_0 + iL_s) \end{cases}$$

$$L_s = s_f \frac{sin\theta}{sin\left(\alpha_f + \theta\right)}$$

Wrapped $V_f = 2\frac{b_f t_f}{s_f} k f_f z\left(cot\theta + cot\alpha_f\right) sin\alpha_f$

k	constant which considers the fibre rupture of the FRP in the round corners of the RC section. k is equal to 0.45 for discontinuous FRP and 0.30 for continuous

---

Monti and Liotta [13]

$$V_{Rd} = min\left(V_{Rd,ct} + V_{Rd,s} + V_{Rd,f}; V_{Rd,max}\right)$$

$$V_{Rd,ct} = \frac{0.18}{\gamma_c} b_w d \cdot min\left(1 + \sqrt{\frac{200}{d}}; 2\right) \sqrt[3]{100 min(\rho_{sl}; 0.02) f_{ck}}$$

$$V_{Rd,s} = 0.9 d f_{yd} \frac{A_{st}}{s_t} (cot\theta + cot\alpha_s) sin\alpha_s$$

θ	Crack angle

For Wrapped or U-shaped configurations: $V_{Rd,f} = \frac{1}{\gamma_{Rd}} 0.9 d f_{fed} \frac{2 t_f w_f}{s_f}\left(cot\theta + cot\alpha_f\right)$

f_{fed}

wrapped

$$f_{fed} = f_{fdd}\left(1 - \frac{1}{6}\frac{L_e sin\alpha_f}{min(0.9d; h_w)}\right) + \frac{1}{2}\left(\phi_R f_{fd} - f_{fdd}\right)\left(1 - \frac{L_e sin\alpha_f}{min(0.9d; h_w)}\right)$$

U-shaped

$$f_{fed} = f_{fdd}\left(1 - \frac{1}{3}\frac{L_e sin\alpha_f}{min(0.9d; h_w)}\right)$$

f_{fdd}	debonding strength	$f_{fdd} = \frac{0.80}{\gamma_{fd}}\sqrt{\frac{2E_f G_f}{t_f}}$
G_f	fracture energy	$G_f = 0.03 k_b \sqrt{f_{ck} f_{ctm}}$
k_b	covering/scale coefficient	$k_b = \sqrt{\frac{2 - w_f/s_f}{1 + w_f/400}} \geq 1$ for strips $k_b = 1$ for continuous sheets
w_f	width measured orthogonally to α_f. w_f should not exceed $min(0.9d; h_w)\, sin\left(\theta + \alpha_f\right)/sin\theta$	
s_f	spacing measured orthogonally to α_f.	
ϕ_R	$\phi_R = 0.2 + 1.6\frac{r_c}{b_w}$, $\quad 0 \leq \frac{r_c}{b_w} \leq 0.5$	

For side-bonded configuration: $V_{Rd,f} = \frac{1}{\gamma_{Rd}} min(0.9d, h_w) f_{fed} \frac{2t_f w_f}{s_f} \frac{sin\alpha_f}{sin\theta}$

f_{fed}

$$f_{fed} = f_{fdd} \frac{z_{rid,eq}}{min(0.9d; h_w)} \left(1 - 0.6\sqrt{\frac{L_e}{z_{rid,eq}}}\right)^2$$

$$z_{rid,eq} = min(0.9d; h_w) - \left(L_e - \frac{s_f}{f_{fdd}/E_f}\right) sin\alpha_f$$

$$V_{Rd,max} = 0.9 d b_w \nu f_{cd} \frac{(cot\theta + cot\alpha_s)}{1 + cot^2\theta}$$

ν $\quad \nu = 0.6(1 - f_{ck}/250)$

Carolin and Täljsten [42]

$$V_f = \eta E_f t_f \varepsilon_{cr} r_f z \frac{sin(\theta + \alpha_f)}{sin\theta}$$

ε_{cr} Critical strain

$$\varepsilon_{cr} = min \begin{Bmatrix} \varepsilon_{f,u} \\ \varepsilon_{bond} sin^2(\theta + \alpha_f) \\ \varepsilon_{c,max} sin^2(\theta + \alpha_f) \end{Bmatrix}$$

$\varepsilon_{f,u}$ Ultimate allowable fibre capacity

ε_{bond} Maximum allowable strain without achieving anchorage

$$\varepsilon_{bond} = \frac{1}{E_f t_f}\sqrt{2E_f t_f G_f} \begin{cases} sin(\omega L_{cr}) & for\ L_{cr} \le \frac{\pi}{2\omega} \\ 1 & for\ L_{cr} > \frac{\pi}{2\omega} \end{cases}$$

G_f Fracture energy

$$\omega = \sqrt{\frac{\tau_{max}^2}{2E_f t_f G_f}}$$

$\varepsilon_{c,max}$ Concrete contribution due to aggregate interlocking. If the concrete contribution is not included in the shear bearing capacity, $\varepsilon_{c,max}$, can be ignored

r_f Factor which depends on the layout of strengthening system

$r_f = sin\alpha_f$ for continuous wrapping

$r_f = \frac{w_f}{s_f}$ for discrete strips

Chen and Teng [23]

$$V_f = 2 f_{f,e} t_f w_f \frac{d_f(cot\theta + cot\alpha_f) sin\alpha_f}{s_f}$$

$f_{f,e}$ Average stress of the FRP intersected by the shear crack

$f_{f,e} = D_f \sigma_{f,max}$

FRP Rupture $\quad D_f = \frac{1 + \zeta}{2}$

$$\zeta = \frac{z_t}{z_b}$$

$$z_t = (0.1d + d_{f,t}) - 0.1d$$

$$z_b = (d - (h - d_f)) - 0.1d$$

	$d_{f,t}$	Distance from the concrete compression face to the actual upper edge of the FRP ($d_{f,t} = 0$ for wrapping)
	$$\sigma_{f,max} = \begin{cases} 0.8f_f & if\ \frac{f_f}{E_f} \leq \varepsilon_{max} \\ 0.8E_f\varepsilon_{max} & if\ \frac{f_f}{E_f} > \varepsilon_{max} \end{cases}$$	
	ε_{max}	1.5% may be used until a soundly proposal is available
FRP Debonding	$$\sigma_{f,max} = min\begin{cases} f_f \\ 0.427\beta_w\beta_L\sqrt{\frac{E_f\sqrt{f_c}}{t_f}} \end{cases}$$	
	$$L_{max} = \begin{cases} \frac{h_f}{sin\beta} & for\ U-jackets \\ \frac{h_f}{2sin\beta} & for\ side\ plates \end{cases}$$	
	$$\beta_L = \begin{cases} 1 & if\ \lambda \geq 1 \\ sin\frac{\pi\lambda}{2} & if\ \lambda < 1 \end{cases}$$	
	$$\lambda = \frac{L_{max}}{L_e}$$	
	$$L_e = \sqrt{\frac{E_f t_f}{\sqrt{f_c}}}$$	
	$\beta_w = \sqrt{\frac{2-w_f/(s_f sin\beta)}{1+w_f/(s_f sin\beta)}}$ for discontinuous sheets	
	$\beta_w = \frac{\sqrt{2}}{2}$ for continuous sheets	

APPENDIX 2. Database of FRP shear-strengthened beams.

Table A2.1. Rectangular beams strengthened in shear by FRP sheets or laminates

Table A2.2 T-beams strengthened in shear by FRP sheets or laminates

NOTATION

b_w = web section width
d = effective depth, that is the distance between the most compressed fibre and the tensile longitudinal reinforcement
f_{ck} = concrete characteristic cylindrical strength
f_{cm} = mean value of the concrete strength
f_{ct} = concrete tensile strength
f_{ctm} = mean value of the concrete tensile strength
f_{fd} = design ultimate strength of the FRP
f_{yd} = design steel yield strength
h_w = height of the web in a T-section
r_c = corner rounding radius
s_t = longitudinal spacing between the internal transverse reinforcement
t_f = thickness of a FRP sheet
w_f = width of a FRP strip
A_{st} = area of transverse internal steel reinforcement, $A_{st} = \frac{n\pi\phi_{st}^2}{4}$

A_f = area of FRP shear reinforcement

E_s = elastic modulus transverse steel

G_f = fracture energy

α_s = angle between the stirrups and the longitudinal axis
γ_c = concrete partial safety coefficient
ϕ_{st} = diameter of the internal transverse reinforcement
ρ_{sl} = longitudinal reinforcement ratio

List of Figures

Figure 1. Experimental vs. theoretical V_f according to Fib Bulletin 90 [1], ACI 440.2R-17 [2], DAfStb [5], CNR-DT-200 R1/2013 [3] and TR-55[4] for rectangular RC beams w/o and with transverse reinforcement for continuous or discnontinous U-shaped, wrapped or side-bonded FRP configurations.

Figure 2. Experimental vs. theoretical V_f according to Fib Bulletin [6], JSCE [51], Rousakis et al. [26], Kotynia [14], and Mofidi and Chaallal [12] for rectangular RC beams w/o and with transverse reinforcement for continuous or discontinuous U-shaped, wrapped or side-bonded FRP configurations.

Figure 3. Experimental vs. theoretical V_f according to Pellegrino and Modena [10,18,53], Monti and Liotta [13], Carolin and Täljsten [42] and Chen and Teng [23], for rectangular RC beams w/o and with transverse reinforcement for continuous or discnontinous U-shaped, wrapped or side-bonded FRP configurations.

Figure 4. Experimental vs. theoretical V_f according to Fib Bulletin 90 [1], ACI 440.2R-17 [2], DAfStb [5], CNR-DT-200 R1/2013 [3] and TR-55[4] for T-RC beams w/o and with transverse reinforcement for continuous or discontinuous U-shaped, wrapped or side-bonded FRP configurations.

Figure 5. Experimental vs. theoretical V_f according to Fib Bulletin 14 [6], JSCE [51], Rousakis et al. [26], Kotynia [14], and Mofidi and Chaallal [12] for T-RC beams w/o and with transverse reinforcement for continuous or discontinuous U-shaped, wrapped or side-bonded FRP configurations.

Figure 6. Experimental vs. theoretical V_f according to Pellegrino and Modena [10,18,53], Monti and Liotta [13], Carolin and Täljsten [42] and Chen and Teng [34], for T-RC beams w/o and with transverse reinforcement for continuous or discontinuous U-shaped, wrapped or side-bonded FRP configurations

Figure 7. Experimental vs. theoretical V_u according to Rousakis et al. [26], Pellegrino and Modena [10,18,53], and Monti and Liotta [13] for rectangular RC beams w/o and with transverse reinforcement for continuous or discontinuous U-shaped, wrapped or side-bonded FRP configurations.

Figure 8. Mean value and dispersion for different θ angles according to different existing models [5], [6], [14], [13], [23] for rectangular RC beams strengthened in a wrapped continuous or discontinuous configuration with and without transverse reinforcement.

Figure 9. Mean value and dispersion for different θ angles according to different existing models [5], [6], [14], [13], [12] [23] for rectangular RC beams strengthened in a wrapped continuous or discontinuous configuration with and without transverse reinforcement.

Figure 10. Influence of the angle of inclination of struts in the different resisting components according to the formulation of Monti and Liotta (2007) [13] for specimens BS2 (Matthys, 2000 [58]) and T4S2-C45 of Deniaud and Cheng (2003) [59].

List of Tables

Table 1. Number of tests with $a/d \geq 2.5$ included in each of the groups considered in the comparative analysis.

Table 2. Particularities of the models considered in the comparative analysis.

Table 3. Statistical results of the experimental to theoretical V_f for rectangular RC beams in a wrapped configuration w/o and w/ transverse reinforcement ($a/d \geq 2.5$).

Table 4. Statistical results of the experimental to theoretical of V_f for RC beam with a T-section in a wrapped configuration w/o and w/ transverse reinforcement ($a/d \geq 2.5$).

Table 5. Statistical results of the experimental to theoretical V_f for rectangular RC beams in a U-shaped configuration w/o and w/ transverse reinforcement ($a/d \geq 2.5$).

Table 6. Statistical results of the experimental to theoretical of V_f for RC beam with a T-section in a U-shaped configuration w/o and w/ transverse reinforcement ($a/d \geq 2.5$).

Table 7. Statistical results of the experimental to theoretical V_f for rectangular RC beams in a side-bonded configuration w/o and w/ transverse reinforcement ($a/d \geq 2.5$).

Table 8. Statistical results of the experimental to theoretical of V_u for RC beam with a rectangular section in a wrapped configuration w/o and w/ transverse reinforcement ($a/d \geq 2.5$).

Table 9. Statistical results of the experimental to theoretical of V_u for RC beam with a rectangular section in a U-shaped configuration w/o and w/ transverse reinforcement ($a/d \geq 2.5$).

Figure 01

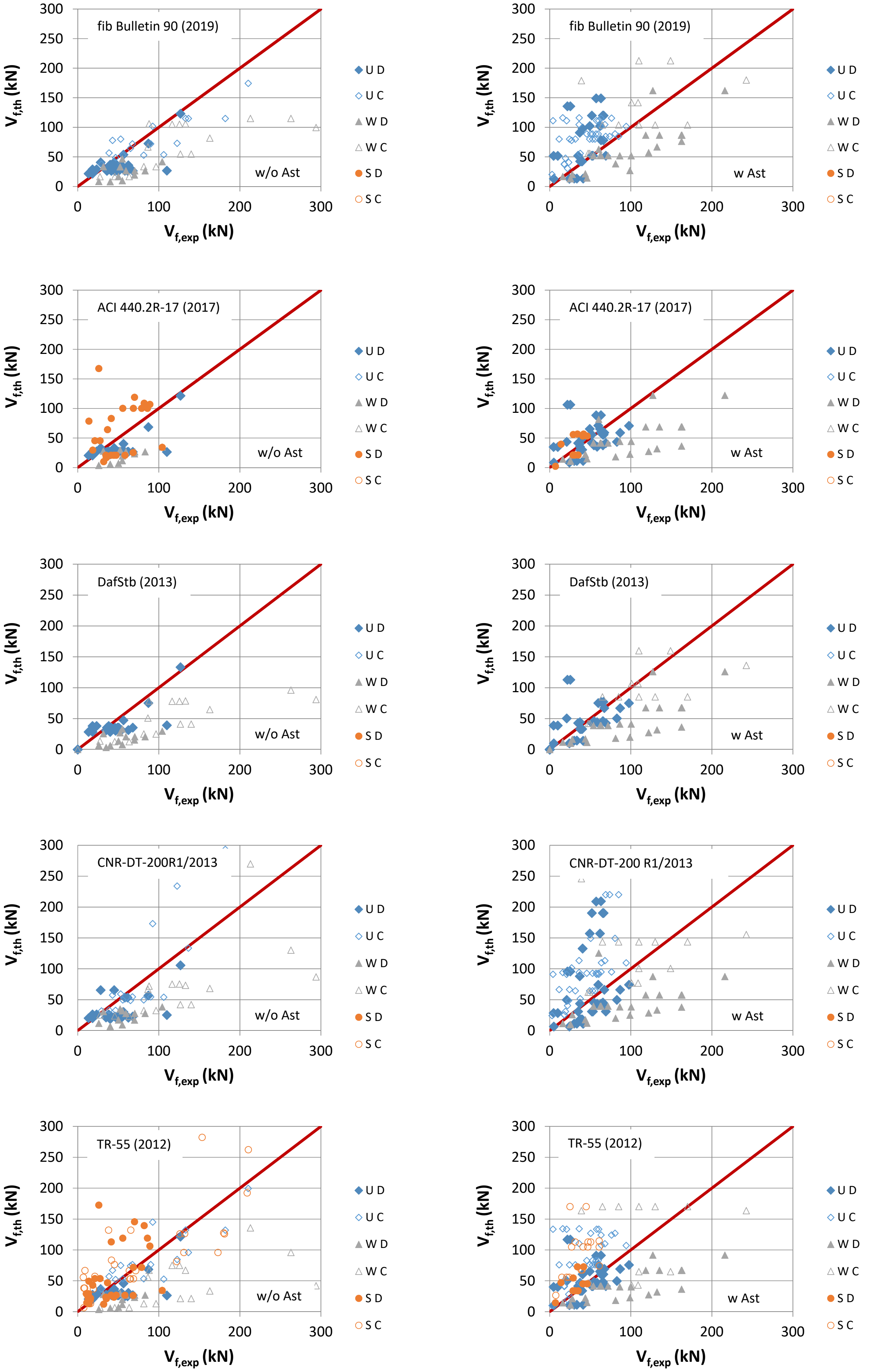
fib Bulletin 90 (2019)
w/o Ast
w Ast
ACI 440.2R-17 (2017)
DafStb (2013)
CNR-DT-200R1/2013
CNR-DT-200 R1/2013
TR-55 (2012)
$V_{f,th}$ (kN)
$V_{f,exp}$ (kN)
U D
U C
W D
W C
S D
S C
0
50
100
150
200
250
300

Figure 02

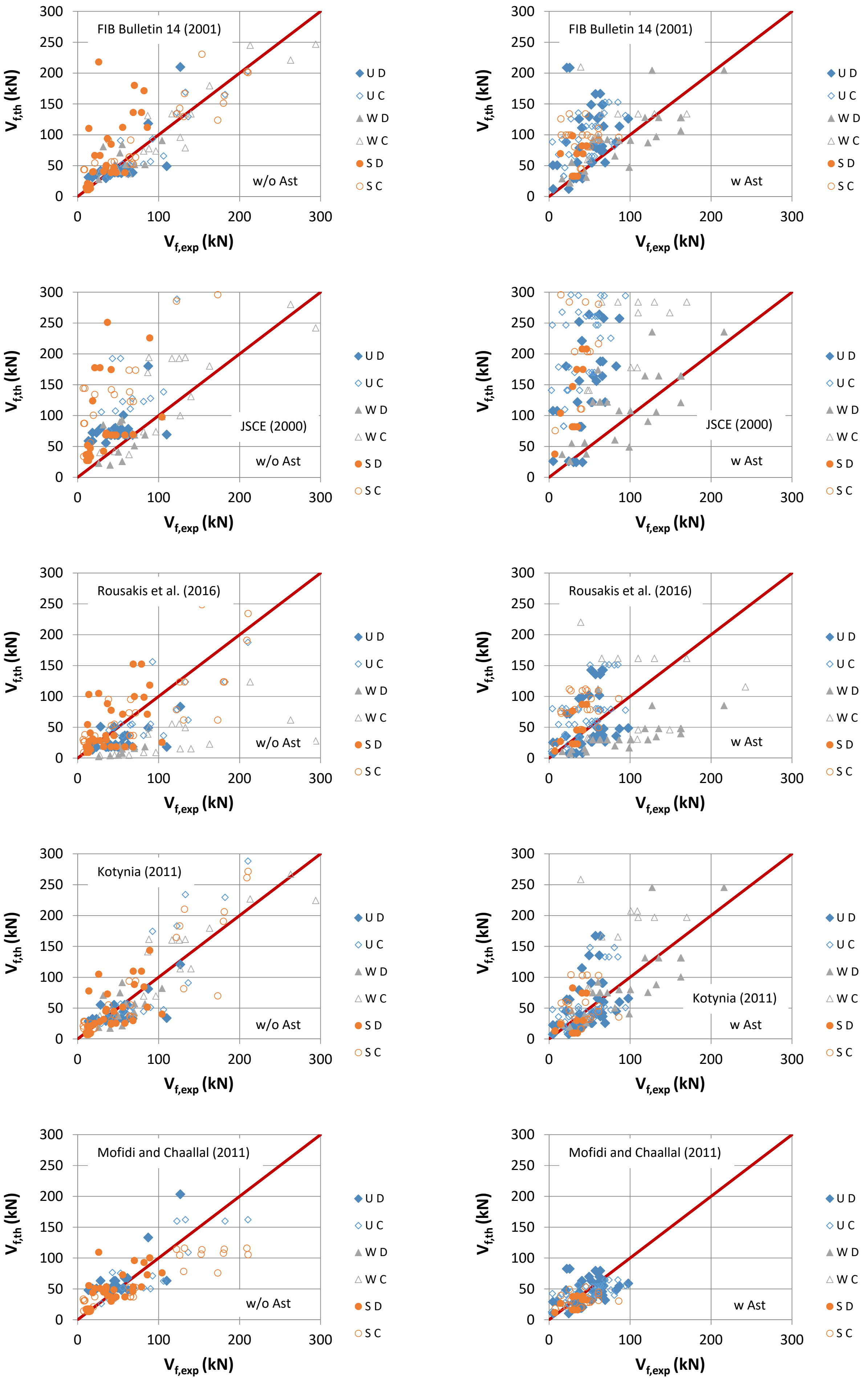
FIB Bulletin 14 (2001)
w/o Ast
w Ast
JSCE (2000)
Rousakis et al. (2016)
Kotynia (2011)
Mofidi and Chaallal (2011)
$V_{f,th}$ (kN)
$V_{f,exp}$ (kN)
0
50
100
150
200
250
300
U D
U C
W D
W C
S D
S C

Figure 03

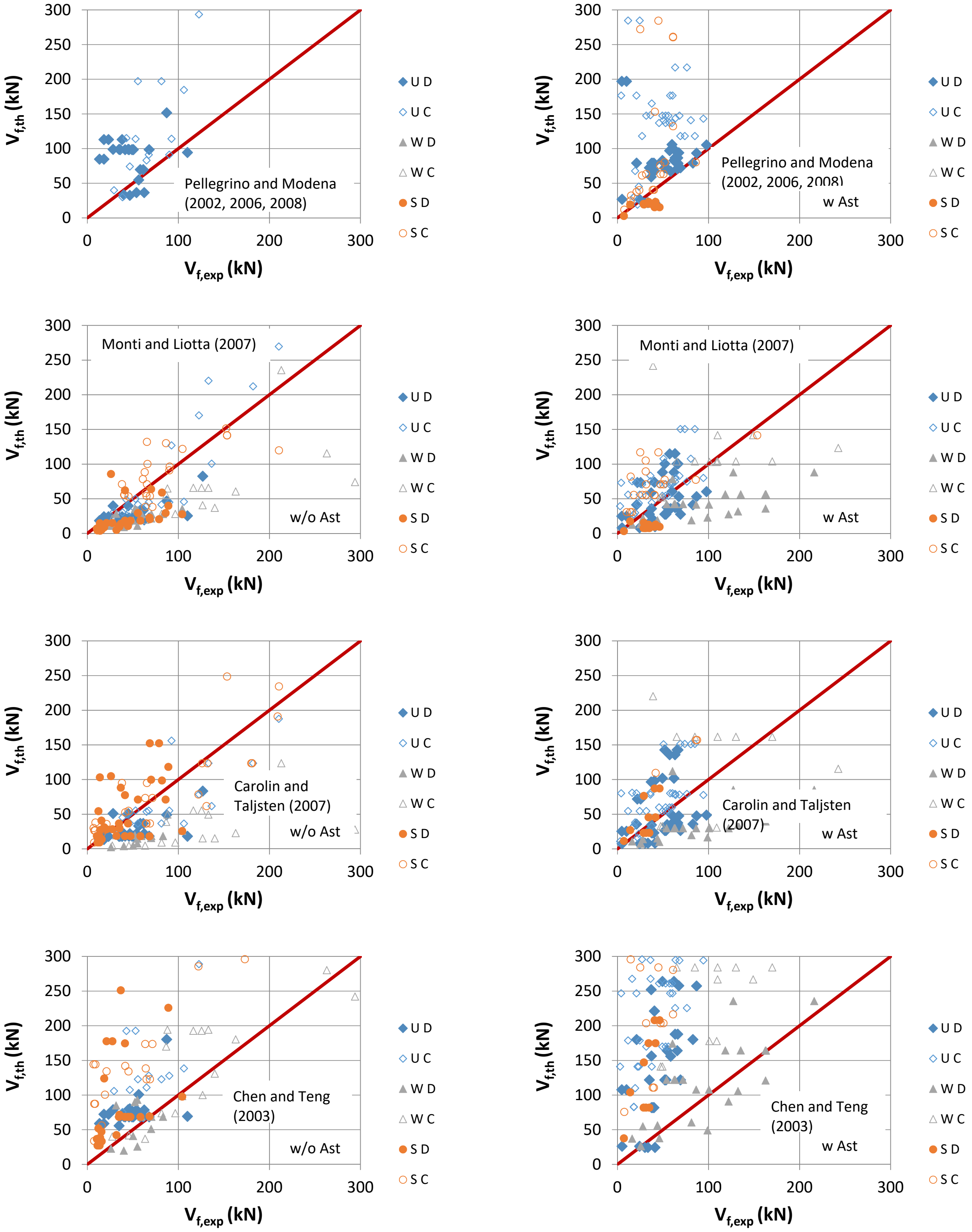

Pellegrino and Modena
(2002, 2006, 2008)
Pellegrino and Modena
(2002, 2006, 2008)
w Ast
Monti and Liotta (2007)
w/o Ast
Monti and Liotta (2007)
w Ast
Carolin and
Taljsten (2007)
w/o Ast
Carolin and Taljsten
(2007)
w Ast
Chen and Teng
(2003)
w/o Ast
Chen and Teng
(2003)
w Ast
$V_{f,th}$ (kN)
$V_{f,exp}$ (kN)
U D
U C
W D
W C
S D
S C
0
100
200
300
0
50
100
150
200
250
300

Figure 04

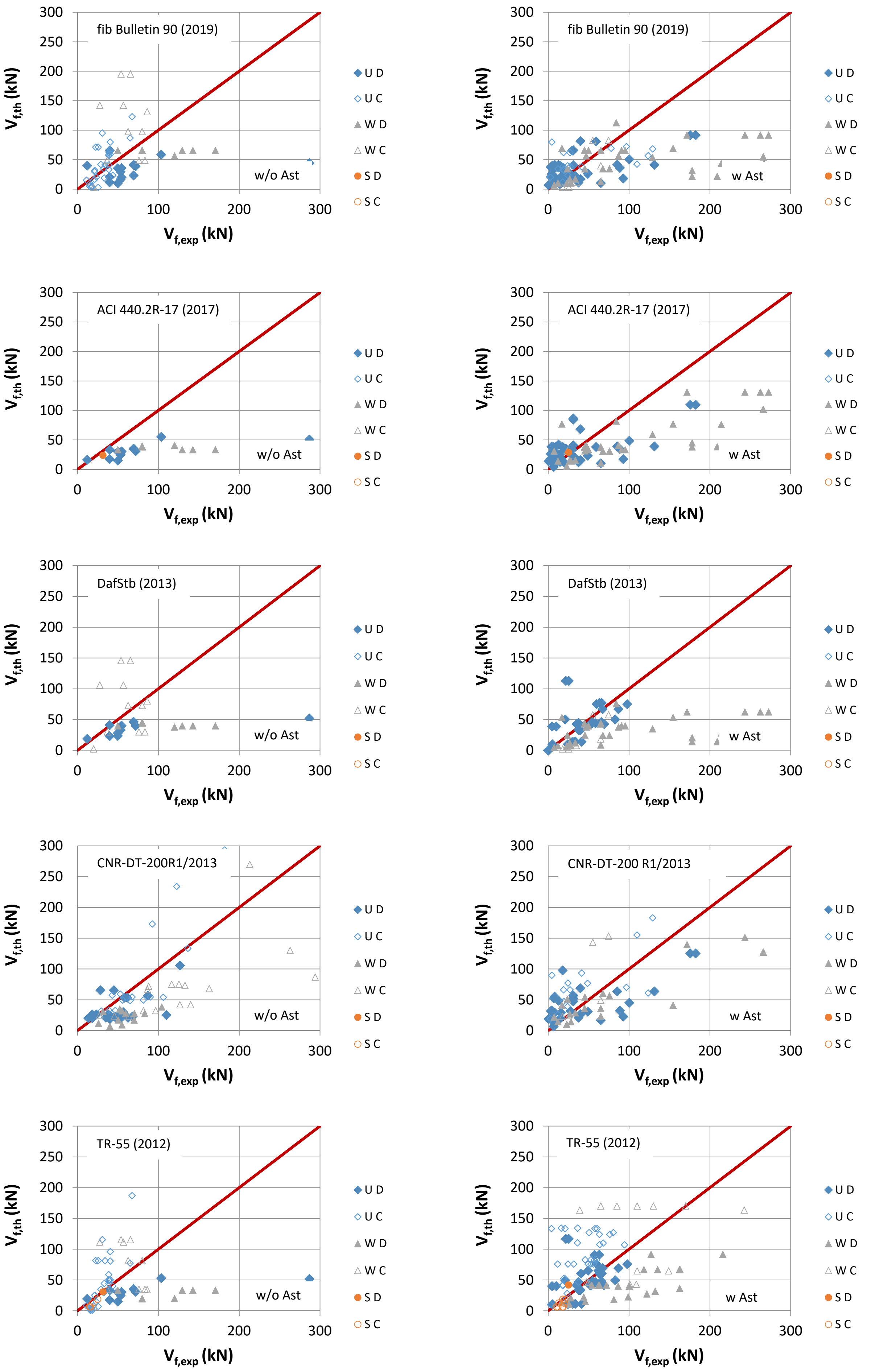
fib Bulletin 90 (2019)
w/o Ast
fib Bulletin 90 (2019)
w Ast
ACI 440.2R-17 (2017)
w/o Ast
ACI 440.2R-17 (2017)
w Ast
DafStb (2013)
w/o Ast
DafStb (2013)
w Ast
CNR-DT-200R1/2013
w/o Ast
CNR-DT-200 R1/2013
w Ast
TR-55 (2012)
w/o Ast
TR-55 (2012)
w Ast
$V_{f,th}$ (kN)
$V_{f,exp}$ (kN)
0
50
100
150
200
250
300
U D
U C
W D
W C
S D
S C

Figure 05

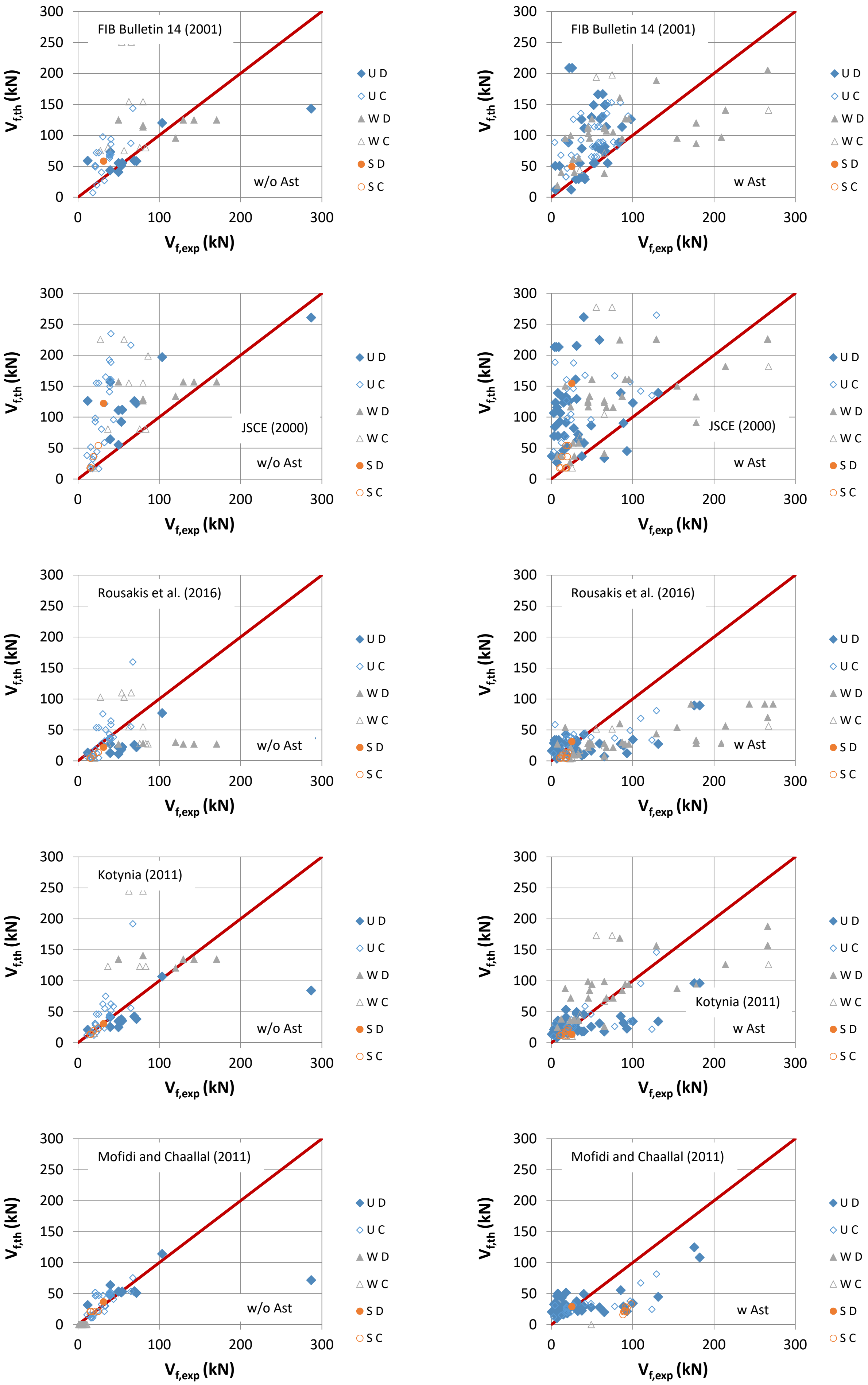

FIB Bulletin 14 (2001)
w/o Ast
w Ast
JSCE (2000)
Rousakis et al. (2016)
Kotynia (2011)
Mofidi and Chaallal (2011)
V f,th (kN)
V f,exp (kN)
0
50
100
150
200
250
300
U D
U C
W D
W C
S D
S C

Figure 06

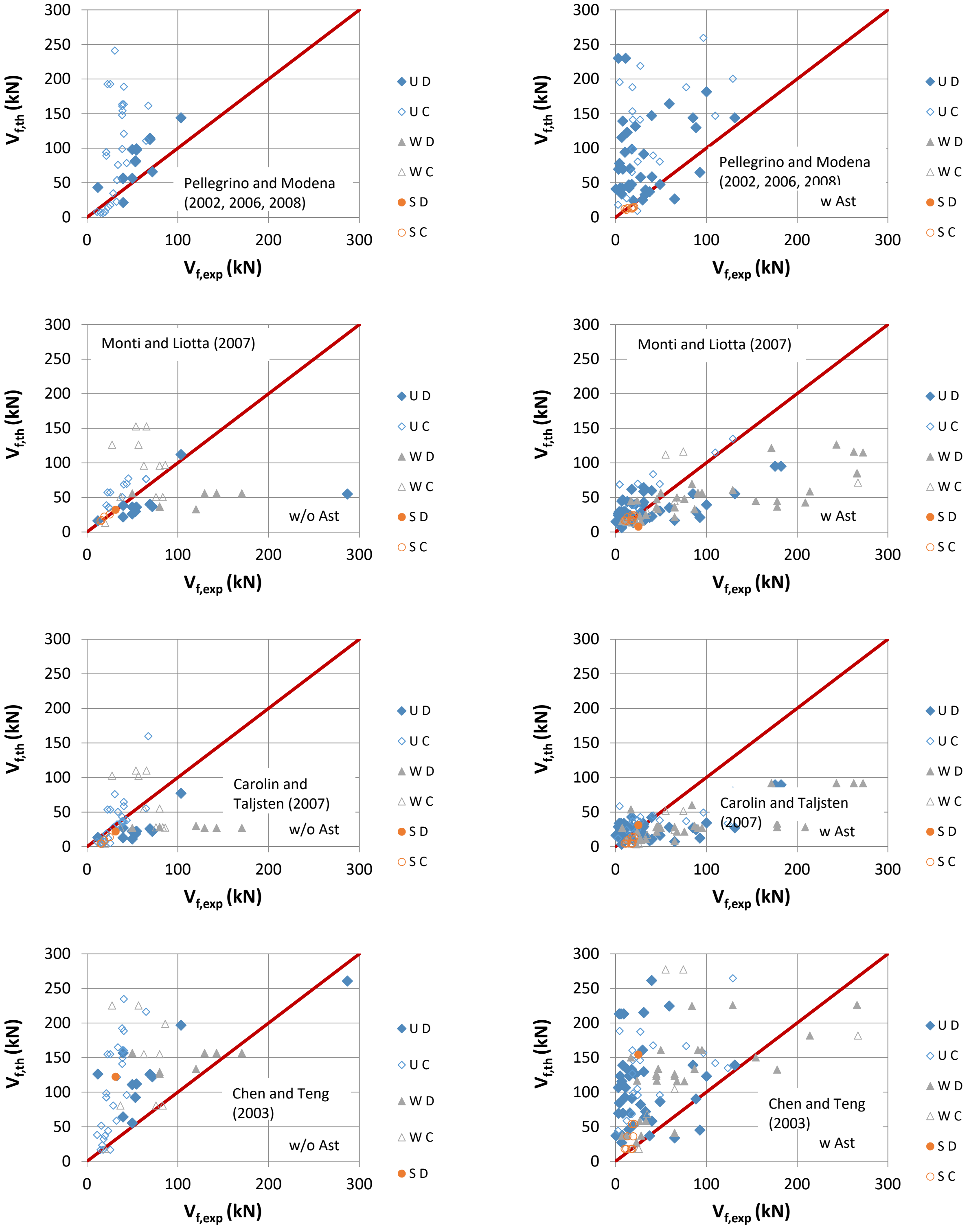

Pellegrino and Modena (2002, 2006, 2008)
Pellegrino and Modena (2002, 2006, 2008)
w Ast
Monti and Liotta (2007)
w/o Ast
Monti and Liotta (2007)
w Ast
Carolin and Taljsten (2007)
w/o Ast
Carolin and Taljsten (2007)
w Ast
Chen and Teng (2003)
w/o Ast
Chen and Teng (2003)
w Ast
$V_{f,th}$ (kN)
$V_{f,exp}$ (kN)
0
50
100
150
200
250
300
U D
U C
W D
W C
S D
S C

Figure 07

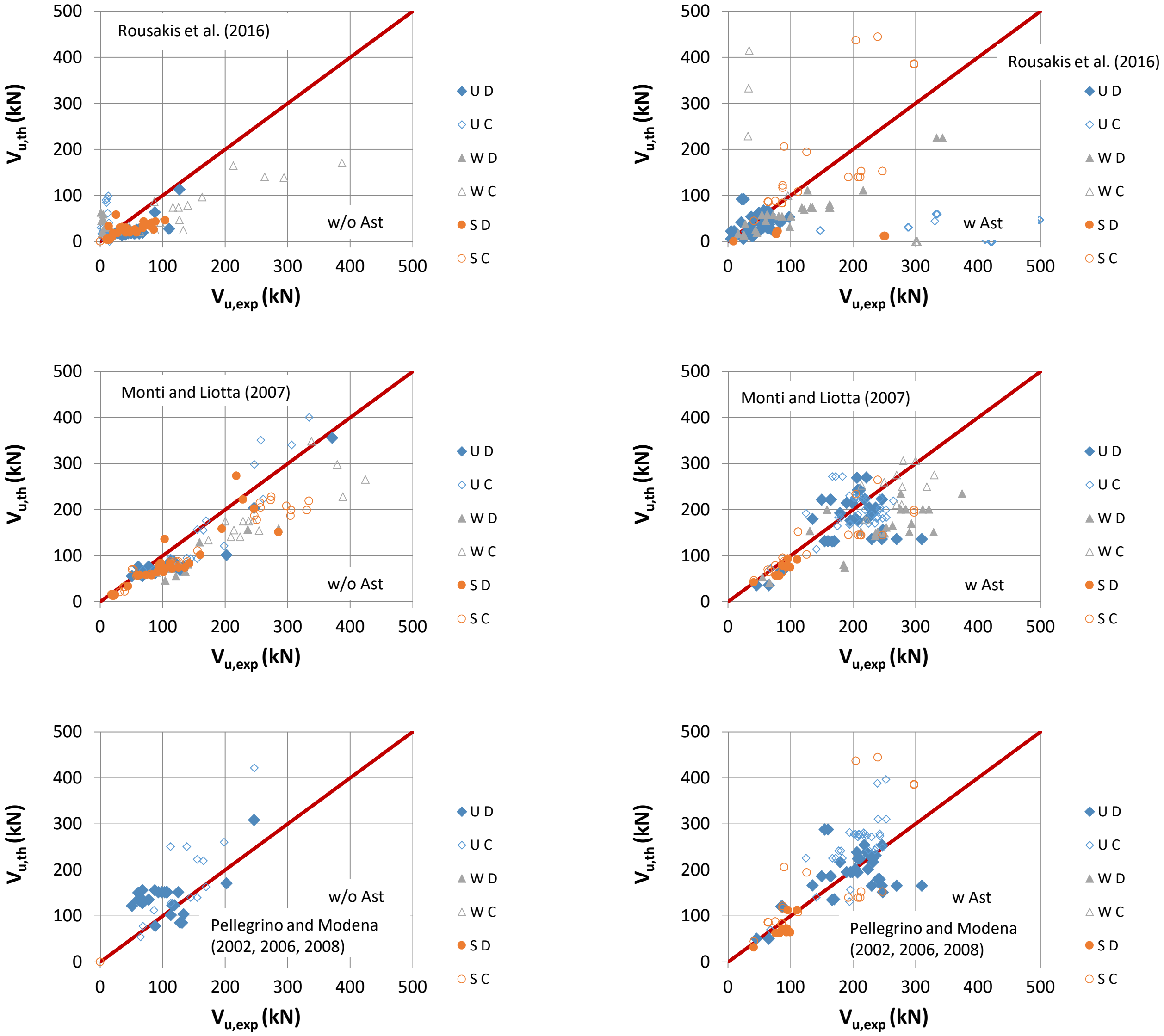
Rousakis et al. (2016)
w/o Ast
w Ast
Monti and Liotta (2007)
Pellegrino and Modena
(2002, 2006, 2008)
$V_{u,th}$ (kN)
$V_{u,exp}$ (kN)
U D
U C
W D
W C
S D
S C
0
100
200
300
400
500

Figure 08

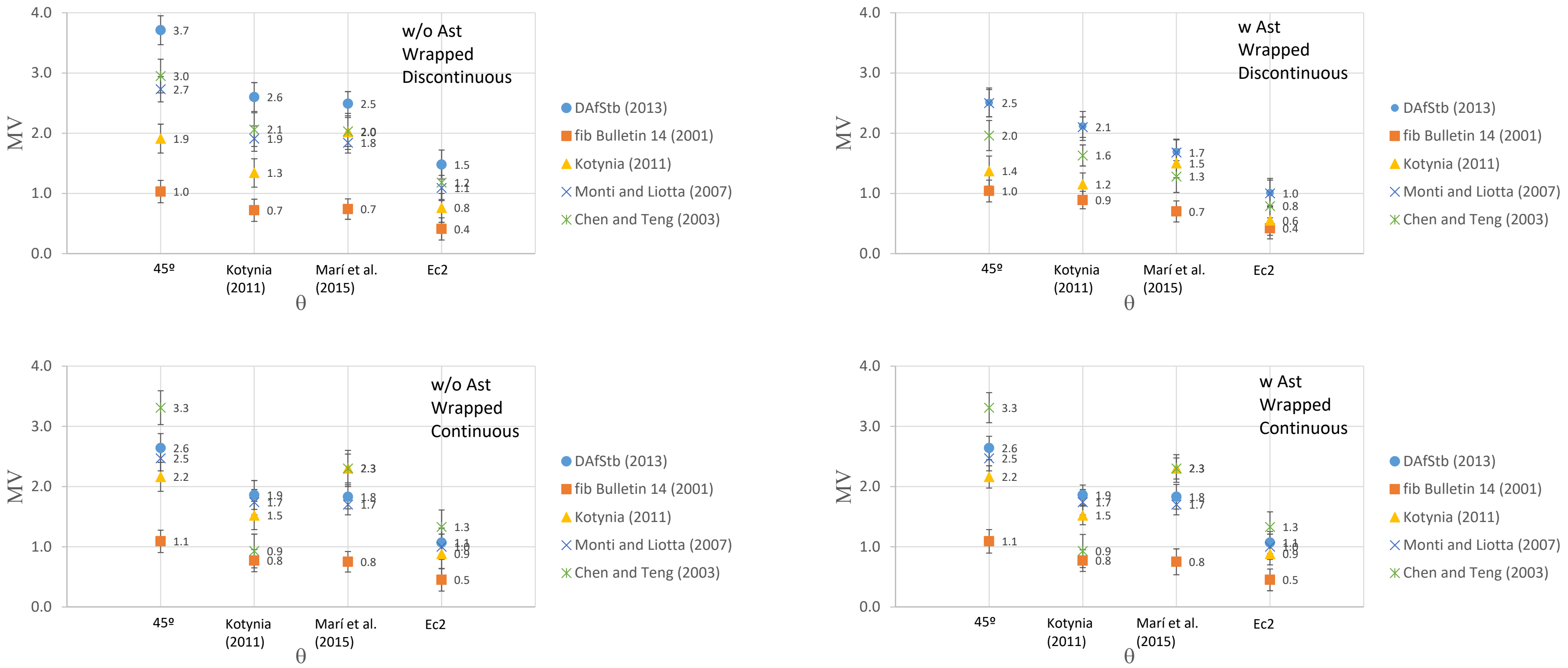

w/o Ast
Wrapped
Discontinuous
w Ast
Wrapped
Discontinuous
w/o Ast
Wrapped
Continuous
w Ast
Wrapped
Continuous
MV
θ
45º
Kotynia (2011)
Marí et al. (2015)
Ec2
DAfStb (2013)
fib Bulletin 14 (2001)
Kotynia (2011)
Monti and Liotta (2007)
Chen and Teng (2003)

Figure 09

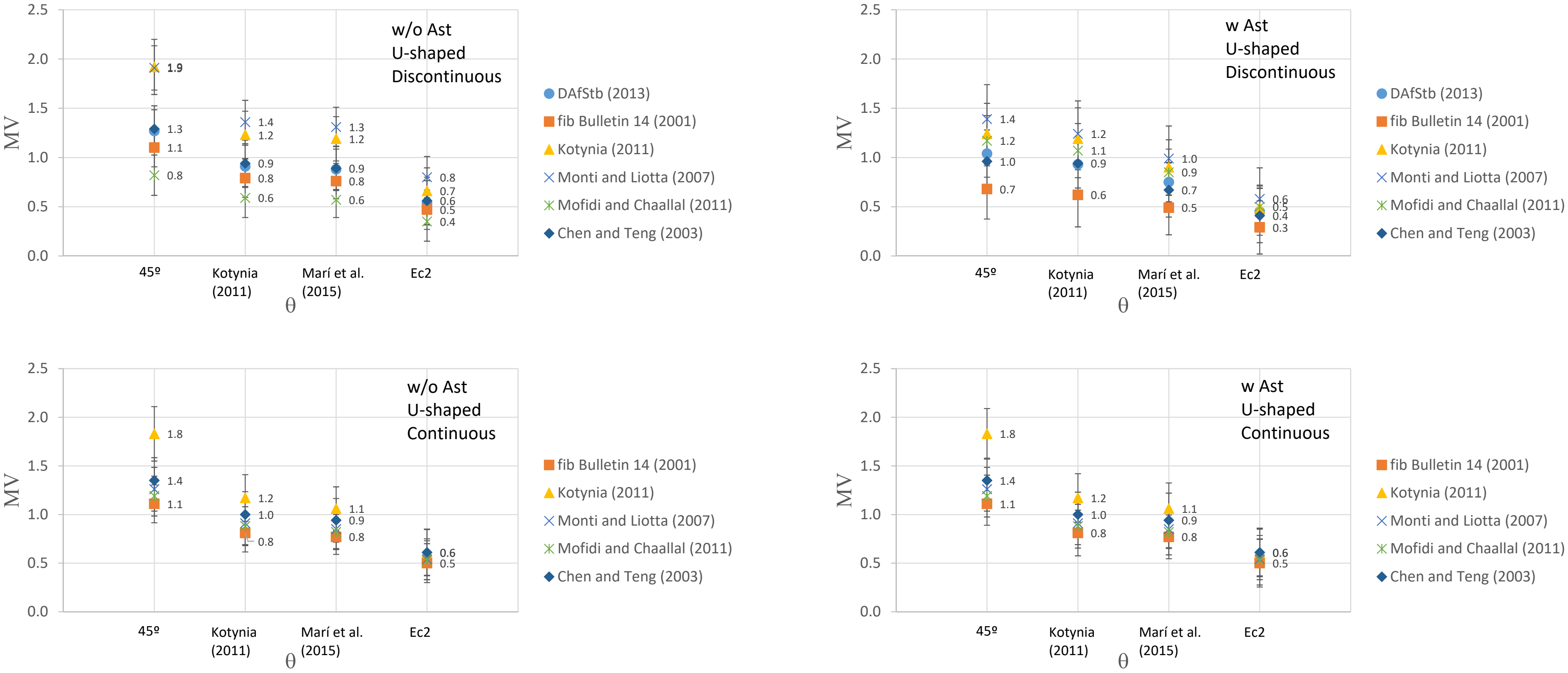
w/o Ast
U-shaped
Discontinuous
w Ast
U-shaped
Discontinuous
w/o Ast
U-shaped
Continuous
w Ast
U-shaped
Continuous
MV
θ
2.5
2.0
1.5
1.0
0.5
0.0
45º
Kotynia (2011)
Marí et al. (2015)
Ec2
DAfStb (2013)
fib Bulletin 14 (2001)
Kotynia (2011)
Monti and Liotta (2007)
Mofidi and Chaallal (2011)
Chen and Teng (2003)

Figure 10a

Click here to access/download;Figure;Figure 10a.jpg

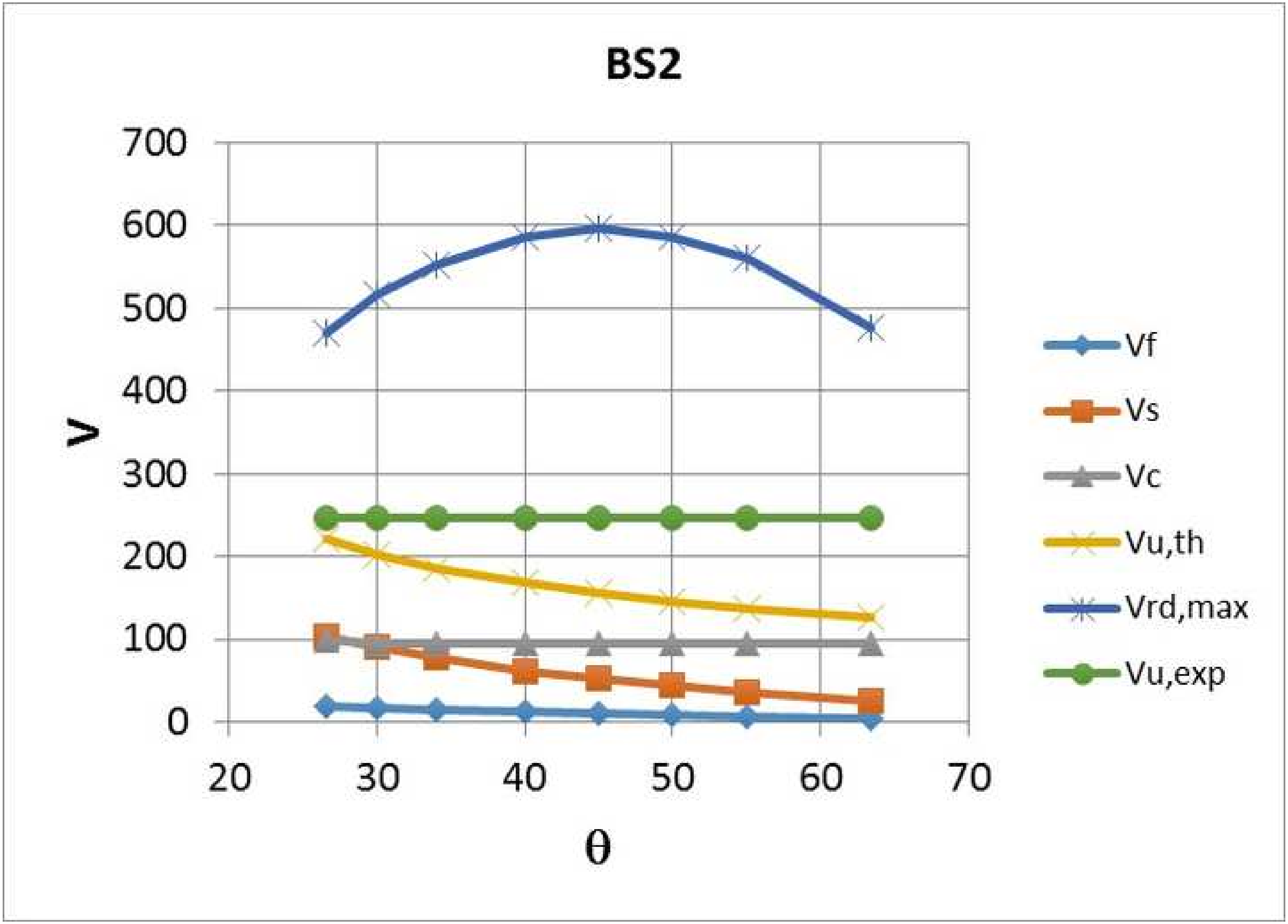

Figure 10b

Click here to access/download;Figure;Figure 10b.jpg

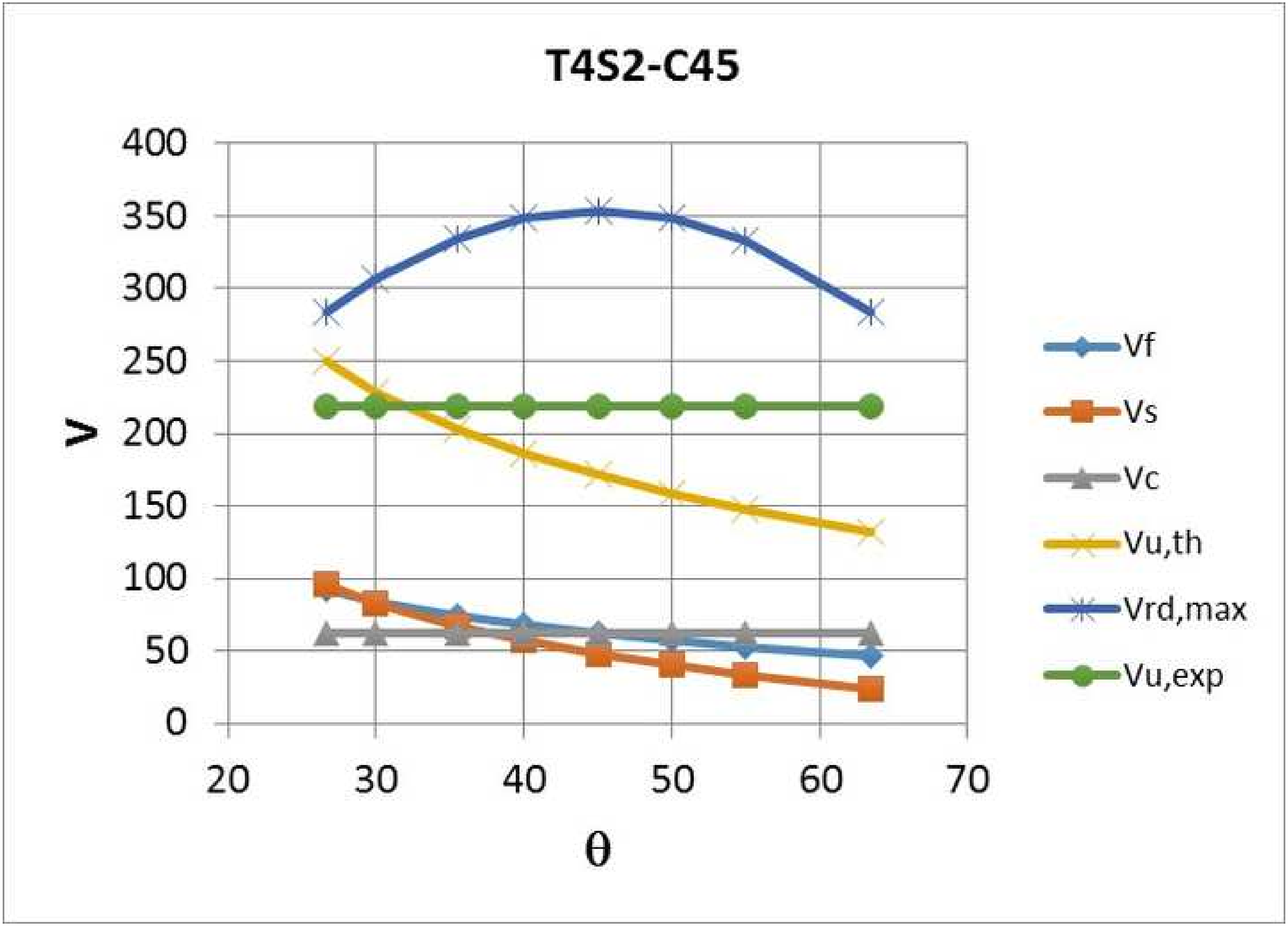

Figure 10c

Click here to access/download;Figure;Figure 10c.jpg

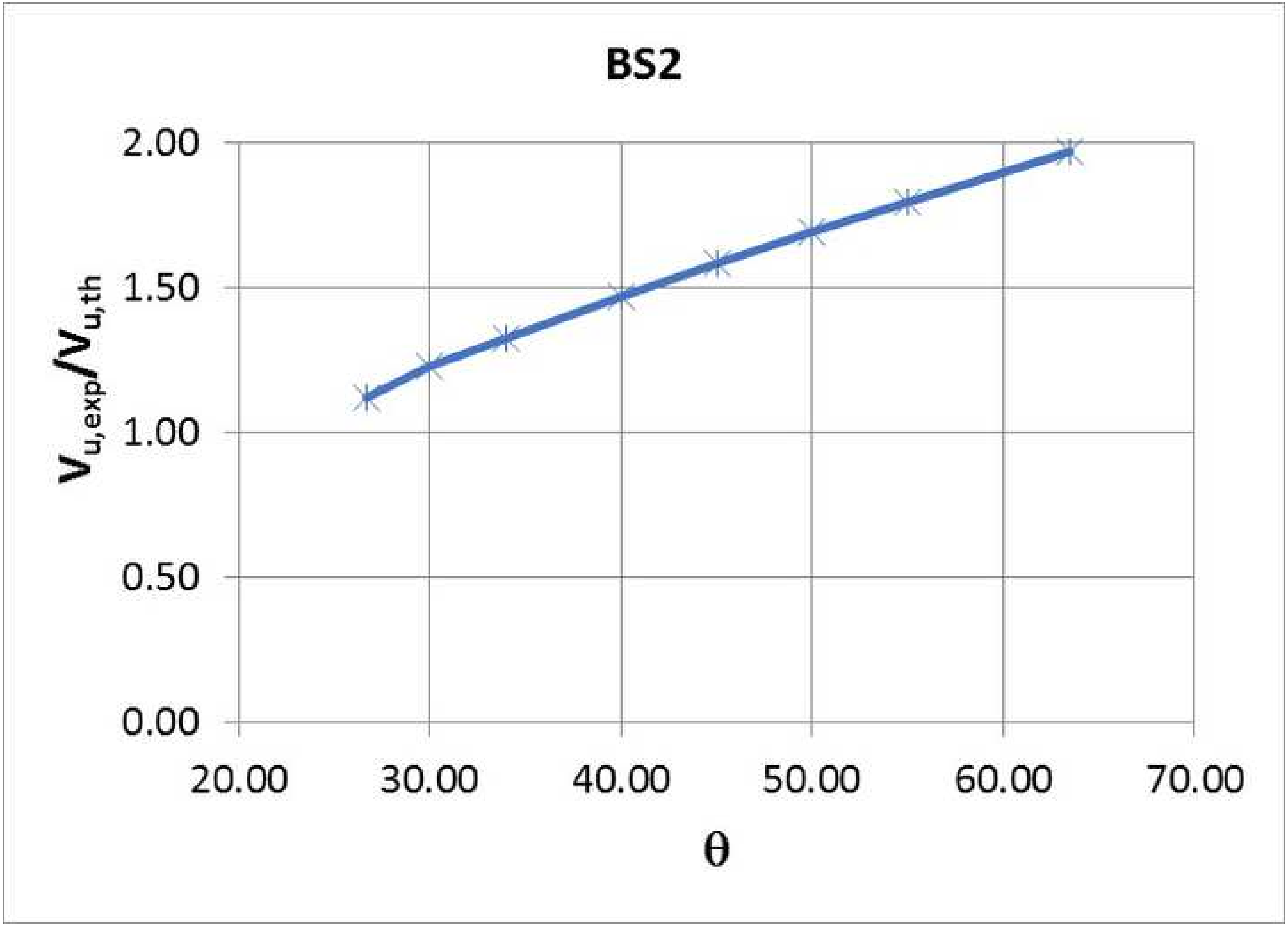

Figure 10d

Click here to access/download;Figure;Figure 10d.jpg

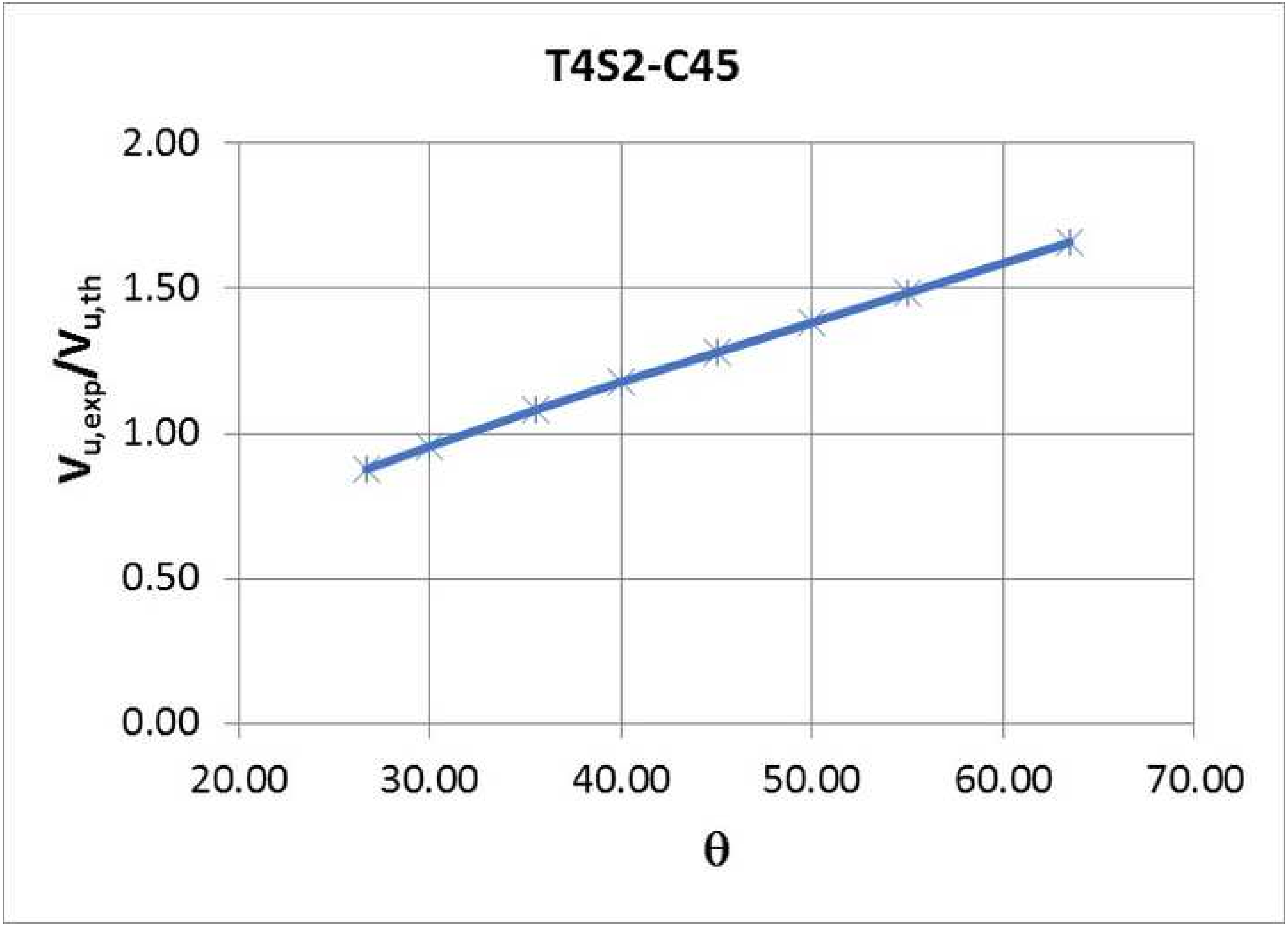

Table 04

Click here to access/download
Table
Table 04.docx

Click here to access/download

Table

Table 05.docx

Click here to access/download
Table
Table 09.docx

Table A2.1

Click here to access/download
Table
Table Appendix 2.1.docx

Table A2.2

Click here to access/download

Table

Table Appendix 2.2.docx